

## Effect of Long-Term Inactivity on Railcar Bearing Lubricant Performance

Constantine Tarawneh, Ph.D.  
Director, UTCRS  
Mechanical Engineering Department  
University of Texas Rio Grande Valley

Jose Jaime Taha, PhD.  
Informatics & Engineering Systems  
University of Texas Rio Grande Valley

Robert Jones, Ph.D.  
Department of Informatics and Engineering Systems  
University of Texas Rio Grande Valley

Douglas Timmer, Ph.D.  
Manufacturing and Industrial Engineering Department  
University of Texas Rio Grande Valley

Kenia Lopez, Melissa Abrego, Adan Serrano, Mia Adame  
Undergraduate Research Assistants  
Mechanical Engineering Department  
University of Texas Rio Grande Valley

A Report on Research Sponsored by

University Transportation Center for Railway Safety (UTCRS)

University of Texas Rio Grande Valley (UTRGV)

June 2026

**Technical Report Documentation Page**

1. Report No. UTCRS-UTRGV-M2CY24	2. Government Accession No.	3. Recipient's Catalog No.	
4. Title and Subtitle  Effect of Long-Term Inactivity on Railcar Bearing Lubricant Performance		5. Report Date June 21, 2026	
		6. Performing Organization Code UTCRS-UTRGV	
7. Author(s) Constantine Tarawneh, Robert Jones, Jose Taha Tijerina, Kenia Lopez, Adan Serrano, Melissa Abrego, and Mia Adame		8. Performing Organization Report No. UTCRS-UTRGV-M2CY24	
9. Performing Organization Name and Address University Transportation Center for Railway Safety (UTCRS) University of Texas Rio Grande Valley (UTRGV) 1201 W. University Dr. Edinburg, TX 78539		10. Work Unit No. (TRAIS)	
		11. Contract or Grant No. 69A3552348340	
12. Sponsoring Agency Name and Address U.S. Department of Transportation (USDOT) University Transportation Centers Program 1200 New Jersey Ave. SE Washington, DC, 20590		13. Type of Report and Period Covered Project Report June 1, 2024 – December 31, 2025	
		14. Sponsoring Agency Code USDOT UTC Program	
15. Supplementary Notes This project is a collaborative effort between UTRGV, NTSB, CSX Transportation, and MxV Rail			
16. Abstract The performance of railroad bearings that sit idle in railyards, large industrial plants, or shipping ports has not been previously explored. Some of the bearings, with documented periods of inactivity exceeding 18 months, have been associated with major derailments. The aforementioned has led to a concern that the inactive periods contributed to early failure, possibly through degradation of the grease properties brought on by moisture intake or grease separation leading to uneven protection of the metal components. The work conducted in collaboration with CSX Transportation and MxV Rail, and in consultation with the National Transportation Safety Board (NTSB), aims to answer the question of whether long-term inactivity has significant effect on bearing performance and service life, and whether these are tied to changes in the lubricant. The performed work consisted of (a) identification of installed bearings on cars that have not moved for periods of three months or longer, (b) removal of the bearings with minimum disruption to the lubricant, (c) pre-test inspection of the still-assembled bearings, (d) installation and service life testing on a laboratory test rig, with continuous performance monitoring of temperature rise, vibration spectra, and power consumption, (e) post-test inspection including disassembly, teardown, and visual inspection of all bearing components, and (f) analysis of the grease composition with specific focus on loss of oxidation inhibitors and evidence of lubricant separation.			
17. Key Words Grease, Lubricants, Roller bearings, Oxidation		18. Distribution Statement This report is available for download from <a href="https://www.utrgv.edu/railwaysafety/research/mechanical/index.htm">https://www.utrgv.edu/railwaysafety/research/mechanical/index.htm</a>	
19. Security Classification (of this report) None	20. Security Classification (of this page) None	21. No. of Pages 88	22. Price

## I. Table of Contents

I.	Table of Contents.....	3
II.	List of Figures.....	4
III.	List of Tables.....	8
IV.	List of Abbreviations.....	9
V.	Disclaimer.....	9
VI.	Acknowledgements.....	9
1	Introduction.....	10
2	Test Setup, Instrumentation, and Measurements.....	11
2.1	Test Axle Setup.....	11
2.2	Instrumentation.....	12
2.2.1	Vibration Sensors.....	12
2.2.2	Temperature Sensors.....	14
2.3	Pre/Post-Test Measurements.....	14
2.3.1	Experiment 282A.....	14
2.3.2	Experiment 283A.....	15
2.3.3	Experiment 304A.....	16
2.3.4	Experiment 304B.....	17
3	Experimental Performance.....	18
3.1	Experiment 282A.....	18
3.1.1	Conditions at Shutdown.....	19
3.1.2	Data Plots.....	19
3.1.3	Test Notes.....	21
3.1.4	Post-Test Teardown and Inspection Pictures.....	24
3.2	Experiment 283A.....	32
3.2.1	Conditions at Shutdown.....	32
3.2.2	Data Plots.....	32
3.2.3	Test Notes.....	34
3.2.4	Post-Test Teardown and Inspection Pictures.....	41
3.3	Experiment 304A.....	49
3.3.1	Conditions at Shutdown.....	49
3.3.2	Data Plots.....	49
3.3.3	Test Notes.....	51
3.3.4	Post-Test Teardown and Inspection Pictures.....	52

3.3.5	Spall Analysis.....	60
3.4	Experiment 304B.....	64
3.4.1	Conditions at Shutdown .....	64
3.4.2	Data Plots .....	65
3.4.3	Test Notes.....	66
3.4.4	Post-Test Teardown and Inspection Pictures .....	66
4	Test Observations .....	71
4.1	Experiment 282A.....	71
4.2	Experiment 283A.....	71
4.3	Experiment 304A.....	76
4.4	Experiment 304B.....	78
5	Grease Analysis Methods .....	79
5.1	Grease Sampling.....	79
5.2	Thermal Analysis (DSC and TGA) .....	80
5.3	Tribology Testing .....	81
5.4	Statistical Analysis .....	82
5.5	Results and Discussion .....	83
5.5.1	Grease Analysis.....	83
5.5.2	Four Ball Wear Testing.....	84
6	Conclusions and Future Work .....	86
7	References.....	88

## II. List of Figures

Figure 1.	Schematic of the bearing setup showing the position of each bearing on the test axle .....	12
Figure 2:	Picture of the UTRGV-UTCRS four bearing tester (4BT) used for this testing .....	12
Figure 3:	Hum Boomerang and Smart Adapter (SA) accelerometer setup.....	13
Figure 4:	Wired accelerometer location in the top-dead-center (TDC) position .....	13
Figure 5:	Temperature sensor instrumentation setup.....	14
Figure 6:	Vibration and temperature above ambient profiles for Exp. 282A .....	20
Figure 7:	Absolute temperature, motor power, and axle RPM profiles for Exp. 282A .....	20
Figure 8:	Applied load profile for Exp.282A.....	21
Figure 9:	Pictures showing grease leak from bearing R4 .....	22
Figure 10:	Pictures of grease accumulation below the inboard (IB) seal of bearing L4.....	23

Figure 11: Pictures of grease accumulation on IB side of bearing L4.....	23
Figure 12: R4 IB cone raceway.....	24
Figure 13: R4 IB cone inner diameter surface .....	24
Figure 14: R4 outboard (OB) cone raceway .....	25
Figure 15: R4 OB cone inner diameter surface.....	25
Figure 16: R4 cup OB raceway on loaded side.....	26
Figure 17: R4 cup IB raceway on loaded side .....	26
Figure 18: R4 IB cone rollers (left) and OB cone rollers (right) .....	27
Figure 19: L4 IB cone raceway showing repaired spall region .....	27
Figure 20: L4 IB cone raceway close-up of repaired spall region .....	28
Figure 21: L4 IB cone inner diameter surface .....	28
Figure 22: L4 OB cone raceway .....	29
Figure 23: L4 OB cone inner diameter surface.....	29
Figure 24: L4 cup IB raceway on loaded side .....	30
Figure 25: L4 cup OB raceway on loaded side.....	30
Figure 26: L4 IB cone rollers (left) and OB cone rollers (right).....	31
Figure 27: Test axle post press-off.....	31
Figure 28: Vibration and temperature above ambient profiles for Exp. 283A .....	32
Figure 29: Absolute temperature, motor power, and axle RPM profiles for Exp. 283A .....	33
Figure 30: Applied load profile of Exp. 283A .....	33
Figure 31: Grease leaking from the IB seal of Bearing L2 (11/05/2024).....	35
Figure 32: Leaked grease accumulation on IB side of Bearing L2 (11/08/2024).....	35
Figure 33: Grease leaking from OB seal of Bearing R2 (11/11/2024) .....	36
Figure 34: Leaked grease accumulation on IB (L2) and OB (R2) sides (11/14/2024) .....	36
Figure 35: Leaked grease accumulation on IB side of Bearing L2 (11/18/2024).....	37
Figure 36: Leaked grease accumulation on IB side of Bearing L2 (12/09/2024).....	37
Figure 37: Leaked grease accumulation on IB (L2) and OB (R2) sides (12/17/2024) .....	38
Figure 38: Leaked grease accumulation on OB (L2) and IB (R2) sides (12/27/2024) .....	38
Figure 39: Leaked grease accumulation on IB (L2) and OB (R2) sides (12/30/2024) .....	39
Figure 40: Leaked grease accumulation on IB (L2) and OB (R2) sides (12/31/2024) .....	39
Figure 41: Leaked grease accumulation on IB (L2) and OB (R2) sides (01/02/2025) .....	40
Figure 42: Leaked grease accumulation on IB (L2) and OB (R2) sides (01/08/2025) .....	40
Figure 43: R2 IB cone raceway.....	41
Figure 44: Small spall (0.015 mm <sup>2</sup> / 0.006 in <sup>2</sup> ) on R2 IB cone raceway .....	41

Figure 45: Close-up of small spall on R2 IB cone raceway .....	42
Figure 46: R2 IB cone inner diameter surface .....	42
Figure 47: R2 OB cone raceway .....	43
Figure 48: R2 OB cone inner diameter surface.....	43
Figure 49: R2 cup OB raceway on loaded side.....	44
Figure 50: R2 cup IB raceway on loaded side .....	44
Figure 51: R2 IB cone rollers (left) and OB cone rollers (right) .....	45
Figure 52: L2 IB cone raceway.....	45
Figure 53: L2 IB cone inner diameter surface .....	46
Figure 54: L2 OB cone raceway .....	46
Figure 55: L2 OB cone inner diameter surface.....	47
Figure 56: L2 cup IB raceway on loaded side .....	47
Figure 57: L2 cup OB raceway on loaded side showing a small pit on the raceway.....	47
Figure 58: Close-up of minor defect on L2 cup OB raceway on loaded side .....	48
Figure 59: L2 IB cone rollers (left) and OB cone rollers (right).....	48
Figure 60: Test axle post press-off.....	49
Figure 61: Vibration and temperature above ambient profiles for Exp. 304A .....	50
Figure 62: Absolute temperature, motor power, and axle RPM profiles for Exp. 304A .....	50
Figure 63: Applied load profile for Exp. 304A.....	51
Figure 64: B2 (12-Month) bearing IB cone raceway .....	53
Figure 65: B2 (12-Month) bearing IB cone inner diameter surface.....	53
Figure 66: B2 (12-Month) bearing OB cone raceway – Picture 1 .....	54
Figure 67: B2 (12-Month) bearing OB cone raceway – Picture 2 .....	54
Figure 68: B2 (12-Month) bearing OB cone raceway – Picture 3 .....	55
Figure 69: B2 (12-Month) bearing OB cone raceway – Picture 4 .....	55
Figure 70: B2 (12-Month) bearing OB cone inner diameter surface .....	56
Figure 71: Orientation convention for cup documentation (view from end-cap side of the test axle) .....	57
Figure 72: B2 (12-Month) bearing cup IB raceway on fan side (0°).....	57
Figure 73: B2 (12-Month) bearing cup IB raceway on loaded side (90°) .....	58
Figure 74: B2 (12-Month) bearing cup IB raceway on non-fan side (180°).....	58
Figure 75: B2 (12-Month) bearing cup IB raceway on unloaded side (270°).....	58
Figure 76: B2 (12-Month) bearing cup OB raceway on fan side (0°) .....	59
Figure 77: B2 (12-Month) bearing cup OB raceway on loaded side (90°).....	59
Figure 78 : B2 (12-Month) bearing cup OB raceway on non-fan side (180°) .....	59

Figure 79: B2 (12-Month) bearing cup OB raceway on unloaded side (270°).....	60
Figure 80: B2 (12-Month) bearing IB cone rollers (left) and OB cone rollers (right).....	60
Figure 81: B2 (12-Month) bearing OB cup spall with an area of 4.57 in <sup>2</sup> (29.48 cm <sup>2</sup> ) (left) and 7.31 in <sup>2</sup> (47.16 cm <sup>2</sup> ) (right) .....	61
Figure 82: B2 (12-Month) bearing OB cone spall with an area of 3.18 in <sup>2</sup> (20.52 cm <sup>2</sup> ) (left) and 3.32 in <sup>2</sup> (21.42 cm <sup>2</sup> ) (right) .....	61
Figure 83: B2 (12-Month) bearing OB cone spall with an area of 3.12 in <sup>2</sup> (20.13 cm <sup>2</sup> ) (left) and 3.96 in <sup>2</sup> (25.55 cm <sup>2</sup> ) (right) .....	62
Figure 84: B2 (12-Month) bearing OB cone spall with an area of 4.41 in <sup>2</sup> (28.45 cm <sup>2</sup> ) (left) and 4.27 in <sup>2</sup> (27.55 cm <sup>2</sup> ) (right) .....	62
Figure 85: B2 (12-Month) bearing OB cone spall with an area of 2.03 in <sup>2</sup> (13.10 cm <sup>2</sup> ) (left) and 0.42 in <sup>2</sup> (2.71 cm <sup>2</sup> ) (right) .....	63
Figure 86: B2 (12-Month) bearing OB cone assembly roller spalls with areas of 1.30 in <sup>2</sup> (8.39 cm <sup>2</sup> ), 1.45 in <sup>2</sup> (9.35 cm <sup>2</sup> ), 2.41 in <sup>2</sup> (15.55 cm <sup>2</sup> ), 0.84 in <sup>2</sup> (5.42 cm <sup>2</sup> ), and 1.07 in <sup>2</sup> (6.90 cm <sup>2</sup> ) [left to right] .....	63
Figure 87: Vibration and temperature above ambient profiles for Exp. 304B.....	65
Figure 88: Absolute temperature, motor power, and axle RPM profiles for Exp. 304B .....	65
Figure 89: Applied load profile for Exp. 304B.....	66
Figure 90: B3 (6-Month) bearing IB cone raceway .....	67
Figure 91: B3 (6-Month) bearing IB cone inner diameter surface.....	67
Figure 92: B3 (6-Month) bearing OB cone raceway .....	68
Figure 93: B3 (6-Month) bearing OB cone inner diameter surface .....	68
Figure 94: B3 (6-Month) bearing cup OB raceway on loaded side .....	69
Figure 95: B3 (6-Month) bearing cup IB raceway on loaded side.....	69
Figure 96: B3 (6-Month) IB cone rollers (left) and OB cone rollers (right).....	70
Figure 97: Test axle post-press-off .....	70
Figure 98: Overview of Bearing L2 OB seal .....	72
Figure 99: Seal weld line of Bearing L2 OB seal .....	73
Figure 100: Grease leak area of Bearing L2 OB seal.....	73
Figure 101: Overview of Bearing R2 IB seal .....	74
Figure 102: Seal weld line of Bearing R2 IB seal.....	74
Figure 103: Grease leak area of Bearing R2 IB seal.....	75
Figure 104: Overview of Bearing R2 OB seal .....	75
Figure 105: Seal weld line of Bearing R2 OB seal .....	76

Figure 106: Grease leak area of Bearing R2 OB seal .....	76
Figure 107: Comparison of the IB cone assembly (left) and OB cone assembly (right) for the B2 (12-Month) bearing .....	78
Figure 108: Exploded view of tapered roller bearing with grease sampling labels (Left Bearing on Axle 4) .....	79
Figure 109: DSC Graphs demonstrate the OIT (left) and the TD (right) of new grease.....	80
Figure 110: Sample TGA output depicting first decomposition step.....	81
Figure 111: R Code for analysis of OIT .....	83
Figure 112. Sample Output from Statistical Model for Decomposition Energy.....	84

### III. List of Tables

Table 1: Pre- and post-test mounted and unmounted lateral spacings for Exp. 282A .....	15
Table 2: Weights of bearings before and after testing and amount of grease loss for Exp. 282A .....	15
Table 3: Test axle press-on and press-off forces for each bearing for Exp. 282A .....	15
Table 4: Pre- and post-test mounted and unmounted lateral spacings for Exp. 283A .....	16
Table 5: Weights of bearings before and after testing and amount of grease loss for Exp. 283A .....	16
Table 6: Test axle press-on and press-off forces for each bearing for Exp. 283A .....	16
Table 7: Pre- and post-test mounted and unmounted lateral spacings for Exp. 304A .....	17
Table 8: Weights of bearings before and after testing and amount of grease loss for Exp. 304A .....	17
Table 9: Test axle press-on and press-off forces for each bearing for Exp. 304A .....	17
Table 10: Pre- and post-test mounted and unmounted lateral spacings for Exp. 304B .....	18
Table 11: Weights of bearings before and after testing and amount of grease loss for Exp. 304B .....	18
Table 12: Test axle press-on and press-off forces for each bearing for Exp. 304B .....	18
Table 13: Timeline of notable events for Exp. 282A.....	22
Table 14: Timeline of notable events for Exp. 283A.....	34
Table 15: Timeline of notable events for Exp. 304A.....	52
Table 16: Bearing B2 Level 2 vibration analysis [3] .....	52
Table 17: B2 (12-Month) bearing spall (damage) area measurements .....	64
Table 18: Timeline of notable events for Exp. 304B.....	66
Table 19: Average OIT, TD, and Weight Loss Values Using Raceway and Seal Samples.....	83
Table 20: Tribological Evaluation Results.....	85

#### **IV. List of Abbreviations**

4BT	Four Bearing Tester
ABD	Acoustic Bearing Detector
AAR	Association of American Railroads
BHI	Bearing Health Index
DSC	Differential Scanning Calorimeter
$G_{rms}$	Root-Mean-Square of the accelerometer output
HBD	Hot Bearing Detector
IB	Inboard
NTSB	National Transportation Safety Board
OB	Outboard
OIT	Oxidation Induction Time
Ref	Reference
RMS	Room-Mean-Square
RPM	Revolutions Per Minute
TD	Thermal Decomposition Energy
TGA	Thermogravimetric Analyzer
USDOT	United States Department of Transportation
UTCRS	University Transportation Center for Railway Safety
UTRGV	University of Texas Rio Grande Valley

#### **V. Disclaimer**

The contents of this report reflect the views of the authors, who are responsible for the facts and the accuracy of the information presented herein. This document is disseminated under the sponsorship of the U.S. Department of Transportation's University Transportation Centers Program, in the interest of information exchange. The U.S. Government assumes no liability for the contents or use thereof.

#### **VI. Acknowledgements**

The authors want to acknowledge the University Transportation Center for Railway Safety (UTCRS) at UTRGV for the financial support provided to perform this study through the USDOT UTC Program under Grant No. 69A3552348340. The authors also wish to acknowledge the support and guidance received by CSX Transportation, MxV Rail, and NTSB. Special thanks are owed to Kim Bowling of CSX Transportation, Matt Wenger of MxV Rail, and Joey Rhine of NTSB.

## 1 Introduction

Little to no information is publicly available on the effects of prolonged inactivity on railroad bearings in rail revenue service. The National Transportation Safety Board (NTSB) investigation into the East Palestine, OH, derailment indicated that the failed bearing that caused the accident had two extended periods of inactivity (565 and 216 days). This observation raised the question of whether prolonged inactivity could cause lubricant degradation, leading to grease separation and compromised bearing performance. To that end, the University Transportation Center for Railway Safety (UTCRS) at the University of Texas Rio Grande Valley (UTRGV), in collaboration with the NTSB, MxV Rail, and CSX Transportation, has undertaken a project to study the effects of long-term inactivity on bearing performance and service life.

In Phase I of this study, CSX Transportation located railcars that sat idle for three years. Before these railcars were scrapped, the bearings were carefully removed from the inactive railcars and handled without rotating the bearings. A total of ten bearings were sent to UTRGV. Four of these bearings were pre-opened and grease collected and analyzed, and the other six bearings remained fully assembled, sealed, and were marked for testing on one of the four-bearing test rigs available at the UTCRS-UTRGV bearing testing facilities. All bearings received at UTRGV were Association of American Railroads (AAR) class F bearings. These bearings were carefully marked based on location on the railcar and their orientation on the axle. Testing was planned in three distinct experiments using two bearings per experiment, with the first experiment completed in June 2024 [1] and subsequent experiments conducted between July 2024 and January 2025.

In parallel, and in an effort to increase the sample size of inactive bearings evaluated in this study, the UTCRS research team prepared a total of three additional bearings that were subjected to outdoor environmental exposure beginning on August 14, 2024. These bearings were assembled using components that had previously accumulated approximately 100,000 miles of service and exhibited no visible wear or defects on the rolling surfaces. Two bearings were fully assembled and remained stationary to simulate inactive storage conditions, while a third bearing was assembled without rollers to allow for increased grease volume and was used exclusively for periodic grease sampling and analysis.

The first bearing was brought indoors on March 1st, 2025, marking six months of exposure to natural elements as part of the study's long-term analysis. The second bearing was subjected to similar idle conditions but was removed after one full year of exposure on August 29, 2025. After removal, both bearings were placed in a controlled laboratory environment at room temperature, maintaining the same orientation as during environmental exposure for subsequent inspection and testing. The bearings remained in the laboratory environment until they were mounted on one of the UTCRS four-bearing test rigs for post-

exposure performance testing. The third bearing was opened every two months for regular grease collection and analysis.

This report discusses the findings from the performance testing and post-test inspection of the final sets of CSX-supplied inactive bearings tested, denoted as L4, R4, L2, and R2, and of the UTCRS bearings that were subjected to six months and one year of outdoor environmental exposure. Grease analysis conducted as part of the broader inactivity study is also included. Collectively, these findings contribute to the ongoing investigation of how prolonged inactivity and environmental exposure may influence railroad bearing performance once returned to service.

## **2 Test Setup, Instrumentation, and Measurements**

### **2.1 Test Axle Setup**

The performance tests were planned for 100,000 miles (161,000 km) where the operating speed and load gradually increased to 66 mph (106 km/h) and 34,400 lbs (153 kN) per bearing, respectively. The test axle setup consisted of two inactive bearings plus two freshly assembled, healthy (defect-free) bearings that served as controls. The schematic of the bearing positions on the test axle is depicted in Figure 1. The tapered-roller bearings were tested at seven velocities and two load conditions to closely replicate field service conditions. The tester (shown in Figure 2) incorporates a hydraulic cylinder capable of applying loads of up to 150% of the full AAR rated load for class F and K railroad bearings. To simulate an unloaded (empty) railcar, 17% of the full AAR rated load is applied, which corresponds to 26 kN (5.85 kips) of load per bearing, whereas a fully loaded railcar (100% load) corresponds to 153 kN (34.4 kips) of load per bearing. Additionally, convective cooling across the bearings was implemented through the incorporation of industrial fans providing a current of air at an average speed of 6.5 m/s (14.5 mph) to mimic the airflow over the bearings when the train is in motion.

For clarity, tests conducted on the UTCRS four-bearing test rig are referenced throughout this report by their assigned experiment numbers (e.g., Experiment 282A, 283A, 304A, and 304B). Although experiments are often discussed in terms of the inactive bearings under investigation (e.g., L4/R4, L2/R2, or the 12-Month and 6-Month bearings), experiment numbers are used when referring to test configuration, instrumentation, and data acquisition, as they correspond to the full four-bearing test setup.

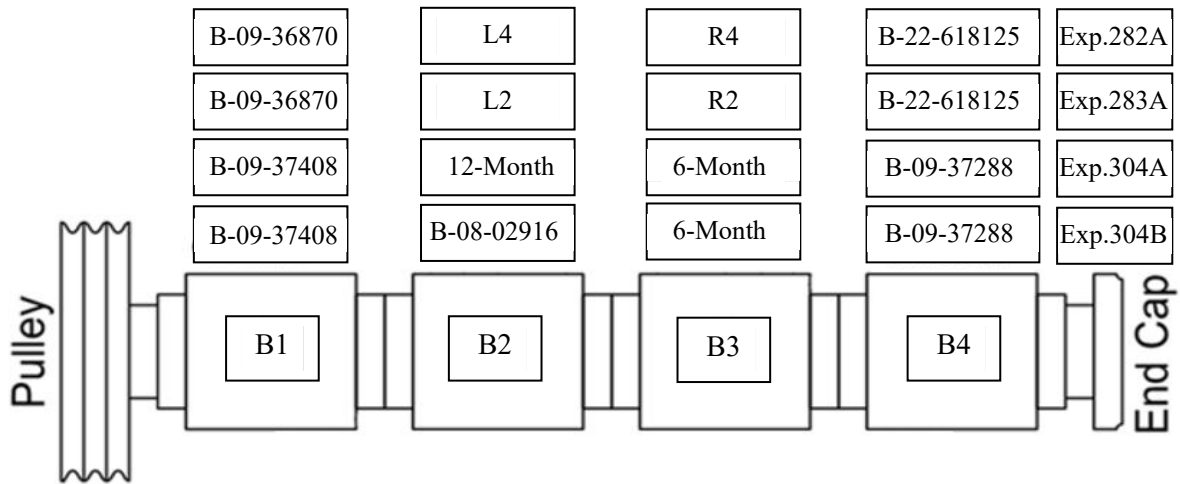


Figure 1. Schematic of the bearing setup showing the position of each bearing on the test axle



Figure 2: Picture of the UTRGV-UTCRS four bearing tester (4BT) used for this testing

## 2.2 Instrumentation

### 2.2.1 *Vibration Sensors*

Two accelerometers monitor and record the vibration levels of each test bearing to assess their condition [2]. Both accelerometers are positioned to measure acceleration along the bearing’s radial direction. The wired accelerometer labeled “Smart Adapter (SA)”, depicted in Figure 3, records data at a frequency of 5.12 kHz for 16 seconds every 10 minutes throughout the duration of the test. For Experiments 282A and 283A, vibration data were collected using both the Hum Boomerang and Smart Adapter accelerometer.

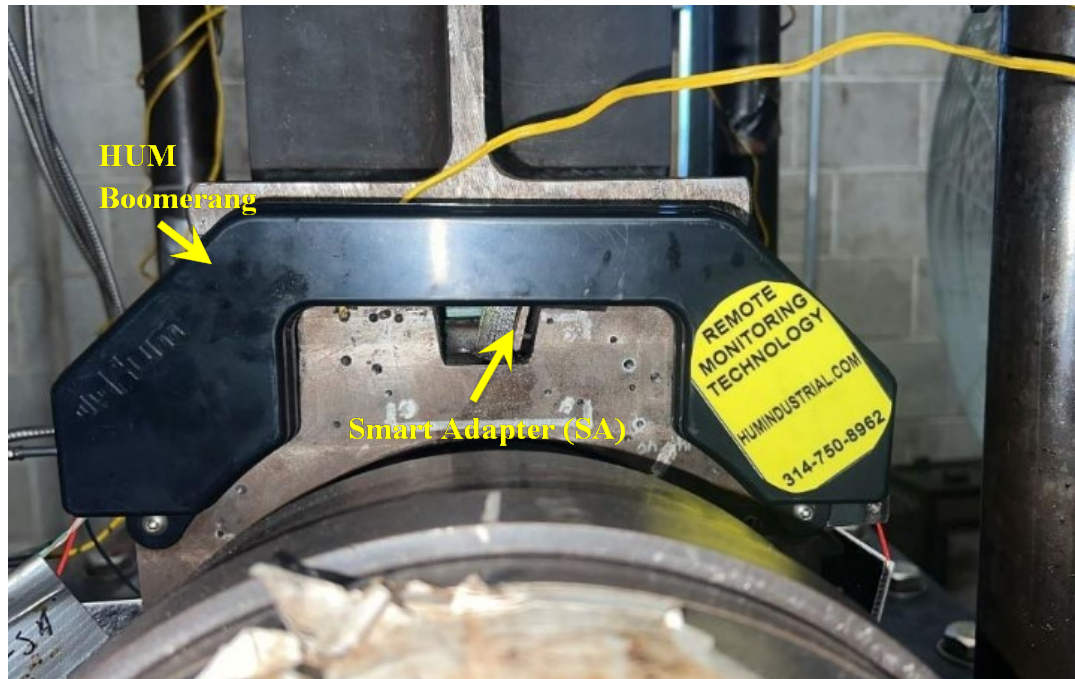


Figure 3: Hum Boomerang and Smart Adapter (SA) accelerometer setup



Figure 4: Wired accelerometer location in the top-dead-center (TDC) position

In Experiments 304A and 304B, a 100-g uniaxial accelerometer monitors and records the vibration levels of each test bearing to assess their condition [3]. The accelerometer, pictured in Figure 4, is positioned to measure acceleration along the bearing's radial direction and records data at a frequency of 5.12 kHz for 16 seconds every 10 minutes throughout the duration of the test.

### 2.2.2 Temperature Sensors

Two bayonet-type (spring-loaded) thermocouples measure the temperatures of the two cup (outer ring) raceways of each test bearing. The bayonet profiles shown in the temperature history plots are the average of the two bayonet thermocouples on each test bearing. An additional K-Type thermocouple is mounted at the same elevation as the bayonet thermocouples using a hose clamp and measures the temperature of the middle of the cup, as shown in Figure 5. An average temperature is calculated for each thermocouple using 50 samples taken at a sampling rate of 100 Hz every 20 seconds. The same temperature sensor configuration and data acquisition settings were used for all experiments discussed in this report.

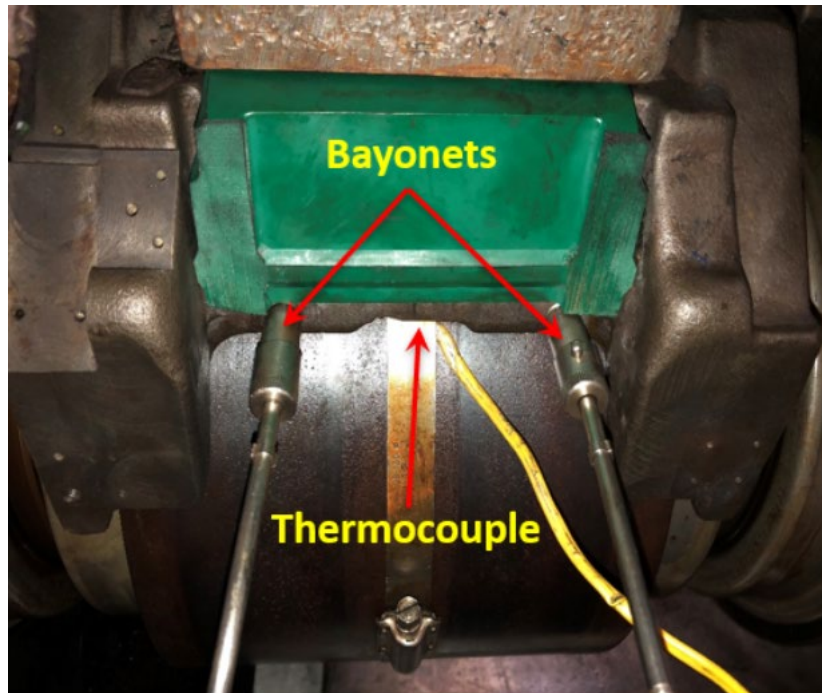


Figure 5: Temperature sensor instrumentation setup

### 2.3 Pre/Post-Test Measurements

Lateral measurements, both mounted and unmounted, pre- and post-test, were taken for each of the bearings following AAR suggested guidelines. These measurements are shown in Table 1, Table 4, Table 7, and Table 10. The “MIN” and “MAX” columns on these tables refer to the minimum and maximum unmounted lateral measurements, respectively. Values of zero for the mounted laterals refer to freely rotating bearings. Table 2, Table 5, Table 8, and Table 11 quantify the amount of grease lost during testing. The percent loss provided is based on 22 oz (623.69 g), which is the total amount of grease packed in a new AAR Class F bearing.

#### 2.3.1 Experiment 282A

The pre- and post-test measurement results for Experiment 283A are summarized in Table 1, Table 2, and Table 3.

Table 1: Pre- and post-test mounted and unmounted lateral spacings for Exp. 282A

Mounted and Unmounted Laterals Pre- and Post-Test								
Bearing	Unmounted Laterals				Mounted Laterals			
	Pre-Test		Post-Test		Pre-test		Post-Test	
	MIN	MAX	MIN	MAX	MIN	MAX	MIN	MAX
B1 - Control	0.025	0.025	0.023	0.024	0.000	0.000	0.000	0.000
B2 – R4	0.013	0.015	0.013	0.015	0.000	0.000	0.000	0.000
B3 – L4	0.016	0.020	0.016	0.020	0.000	0.000	0.000	0.000
B4 - Control	0.025	0.026	0.025	0.026	0.000	0.001	0.000	0.001

Table 2: Weights of bearings before and after testing and amount of grease loss for Exp. 282A

Bearing	Bearing Weights [lbs]		Grease Loss		
	Pre-Test	Post-Test	[oz]	[g]	% Loss
B1 - Control	79.22	79.20	0.32	9.07	1.5
B2 – R4	82.28	82.25	0.48	13.61	2.2
B3 – L4	81.97	81.94	0.48	13.61	2.2
B4 - Control	79.09	79.07	0.32	9.07	1.5

The bearings are pressed onto the axle starting with Bearing B4 and ending with Bearing B1 and are pressed off in reverse order. A modified cone (inner ring) with a larger inner diameter is used to initiate bearing press off and the press-off value represents the initial force required to break static friction for all four bearings. Table 3 lists the press-on and press-off forces for each bearing.

Table 3: Test axle press-on and press-off forces for each bearing for Exp. 282A

Bearing	Press Forces			
	Press On		Press Off	
	[kips]	[kN]	[kips]	[kN]
Cone (Press Off only)	--	--	401.3	1785.1
B4 - Control	64.6	287.4	274.6	1221.5
B3 - L4	108.0	480.4	268.7	1195.2
B2 - R4	203.3	904.3	207.5	923.0
B1 - Control	375.5	1670.3	128.4	571.2

### 2.3.2 Experiment 283A

The pre- and post-test measurement results for Experiment 283A are summarized in Table 4, Table 5, and Table 6.

Table 4: Pre- and post-test mounted and unmounted lateral spacings for Exp. 283A

Mounted and Unmounted Laterals Pre- and Post-Test								
Bearing	Unmounted Laterals				Mounted Laterals			
	Pre-Test		Post-Test		Pre-test		Post-Test	
	MIN	MAX	MIN	MAX	MIN	MAX	MIN	MAX
B1 - Control	0.025	0.026	N/A	N/A	0.000	0.000	0.000	0.000
B2 – R2	0.012	0.015	0.012	0.014	0.000	0.000	0.000	0.000
B3 – L2	0.017	0.018	0.000	0.001	0.000	0.000	0.000	0.000
B4 - Control	0.025	0.026	N/A	N/A	0.000	0.001	0.000	0.000

Table 5 shows that the B1 and B4 bearings experienced weight reductions of 1.15 lbs and 2.38 lbs, respectively. These reductions were due to the intentional cutting of the bearing seals to facilitate bearing removal from the axle. As a result, the exact amount of grease loss could not be quantified, and post-test unmounted lateral measurements in Table 4 were not obtained. However, these two bearings were only used as healthy control bearings and not intended for performance testing.

Table 5: Weights of bearings before and after testing and amount of grease loss for Exp. 283A

Bearing	Bearing Weights [lbs]		Grease Loss		
	Pre-Test	Post-Test	[oz]	[g]	% Loss
B1 – Control	79.29	78.14	N/A	N/A	N/A
B2 – R2	79.14	78.94	3.20	90.72	14.5
B3 – L2	81.96	81.81	2.40	68.04	10.9
B4 – Control	79.10	76.72	N/A	N/A	N/A

Table 6: Test axle press-on and press-off forces for each bearing for Exp. 283A

Bearing	Press Forces			
	Press On		Press Off	
	[kips]	[kN]	[kips]	[kN]
Cone (Press Off only)	--	--	429.5	1910.7
B4 – Control	56.7	252.2	1.3	5.8
B3 – L2	129.7	576.9	22.4	99.6
B2 – R2	200.6	892.3	222.6	990.2
B1 – Control	262.1	1165.9	292.2	1299.8

### 2.3.3 Experiment 304A

Table 7, Table 8, and Table 9 summarize the pre- and post-test measurement results for Experiment 304A. Following termination of the test, bearings B1 and B2 were pressed off the axle due to the observed conditions of B2, while bearings B3 and B4 remained mounted to allow continued evaluation in a subsequent experiment. Consequently, post-test measurements were not obtained for the bearings that remained on the axle. The post-test unmounted lateral measurements for bearing B2 in Table 7 were higher

than typical values, likely due to raceway damage that developed during the experiment and altered internal bearing clearances. The observed operating behavior of bearing B2 during testing is discussed in detail in Section 3.4.

Table 7: Pre- and post-test mounted and unmounted lateral spacings for Exp. 304A

Bearing	Unmounted Laterals [in]				Mounted Laterals [in]			
	Pre-Test		Post-Test		Pre-test		Post-Test	
	MIN	MAX	MIN	MAX	MIN	MAX	MIN	MAX
B1 – Control	0.025	0.026	0.017	0.018	0.001	0.002	0.000	0.000
B2 – 12-Month	0.021	0.022	0.034	0.035	0.000	0.000	0.003	0.005
B3 – 6-Month	0.023	0.025	N/A	N/A	0.000	0.000	N/A	N/A
B4 – Control	0.020	0.022	N/A	N/A	0.000	0.000	N/A	N/A

Table 8: Weights of bearings before and after testing and amount of grease loss for Exp. 304A

Bearing	Bearing Weights [lbs]		Grease Loss		
	Pre-Test	Post-Test	[oz]	[g]	% Loss
B1 – Control	79.03	79.03	0.00	0.00	0.0
B2 – 12-Month	79.44	79.29	2.40	68.04	10.9
B3 – 6-Month	79.25	N/A	N/A	N/A	N/A
B4 – Control	79.04	N/A	N/A	N/A	N/A

Table 9: Test axle press-on and press-off forces for each bearing for Exp. 304A

Bearing	Press Forces			
	Press On		Press Off	
	[kips]	[kN]	[kips]	[kN]
Cone (Press Off only)	--	--	386	1717.0
B4 – Control	38.0	169.1	N/A	N/A
B3 – 6-Month	80.0	356.0	N/A	N/A
B2 – 12-Month	141.0	627.5	222.0	987.9
B1 – Control	190.0	845.5	231.0	1028.0

#### 2.3.4 Experiment 304B

Table 10, Table 11, and Table 12 provide a summary of the pre- and post-test measurement results for Experiment 304B. The pre-test unmounted, mounted, and weight measurements reported for bearings B3 and B4 in Table 10 and Table 11 correspond to the same values documented for Experiment 304A, since the bearings were not removed between experiments.

Table 10: Pre- and post-test mounted and unmounted lateral spacings for Exp. 304B

Bearing	Unmounted Laterals				Mounted Laterals			
	Pre-Test		Post-Test		Pre-test		Post-Test	
	MIN	MAX	MIN	MAX	MIN	MAX	MIN	MAX
B1 – Control	0.028	0.028	0.012	0.013	0.000	0.001	0.000	0.001
B2 – Control	0.023	0.027	0.013	0.017	0.000	0.000	0.000	0.000
B3 – 6-Month	0.023	0.025	0.012	0.013	0.000	0.000	0.000	0.000
B4 – Control	0.020	0.022	0.008	0.012	0.000	0.000	0.000	0.000

Table 11: Weights of bearings before and after testing and amount of grease loss for Exp. 304B

Bearing	Bearing Weights [lbs]		Grease Loss		
	Pre-Test	Post-Test	[oz]	[g]	% Loss
B1 – Control	79.01	79.01	0.00	0.00	0.0
B2 – Control	79.04	79.04	0.00	0.00	0.0
B3 – 6-Month	79.25	79.20	0.80	22.68	3.6
B4 – Control	79.04	79.04	0.00	0.00	0.0

Press-on forces for bearings B3 and B4 are not provided, as these bearings remained mounted on the test axle following Experiment 304A.

Table 12: Test axle press-on and press-off forces for each bearing for Exp. 304B

Bearing	Press Forces			
	Press On		Press Off	
	[kips]	[kN]	[kips]	[kN]
Cone (Press Off only)	--	--	508	2259.7
B4 – Control	N/A	N/A	342	1521.3
B3 – 6-Month	N/A	N/A	332	1476.8
B2 – Control	163	725.1	195	867.4
B1 – Control	198	880.7	96	427.0

### 3 Experimental Performance

The performance tests discussed in this section were planned for a target mileage of 100,000 miles (160,934 kilometers), as determined through discussions with all project partners. The following subsections summarize the results of each experiment and the post-test condition of the bearings.

#### 3.1 Experiment 282A

Experiment 282A ran a total of 100,085 miles (161,071 kilometers), achieving the target mileage with no evidence of bearing defect initiation. A full teardown and inspection of all four bearings involved in this test was subsequently performed.

### 3.1.1 Conditions at Shutdown

- Applied Load: **100% load**, which is equivalent to an AAR Class F load rating of 34.4 kips (153 kN) per bearing. Note that, since the load was applied over the two middle bearings, a total of 68.8 kips (306 kN) was applied resulting in 34.4 kips (153 kN) on each test bearing.
- Axle Rotational Speed: **618 RPM**
- Equivalent Train Traveling Velocity: **66 mph (106 km/h)**
- Average Ambient Temperature: **22.2 °C**
- Total Distance Traveled: **100,085 mi (161,071 km)**
- Percentage of 100k Mile Target Distance: **100.1%**
- Average Air Convection Speed Over Bearings: **14.5 mph (23 km/h)**

### 3.1.2 Data Plots

The vibration and temperature-above-ambient profiles are provided in Figure 6. Figure 7 presents the absolute temperature, motor power, and axle rotational speed profiles, while Figure 8 presents the applied load profiles for this test.

The solid blue and red lines shown in the vibration profile plot in Figure 6 represent the “Prelim. Threshold” and “Maximum Threshold”, respectively. These thresholds are based on statistical analysis of the extensive library of bearing vibration data at the UTCRS. The preliminary threshold is used to differentiate between healthy bearings and possibly defective bearings. In other words, bearings with vibration levels that are lower than the preliminary threshold (solid blue line) are healthy (defect-free) bearings, whereas bearings with vibration levels above the preliminary threshold are possibly defective. If a bearing’s vibration levels are above the maximum threshold (solid red line), then that bearing is defective with a 97% confidence level [3]. The solid orange line in the temperature profile plot represents the maximum average bearing operating temperature-above-ambient for healthy bearings at the respective speed and load condition. The solid red line represents the recommended AAR Hot Bearing Detector alarm threshold, which is 170°F (94.4°C) above ambient conditions. The data plots presented in the subsequent experiment sections use the same thresholds and reference lines as described in this section.

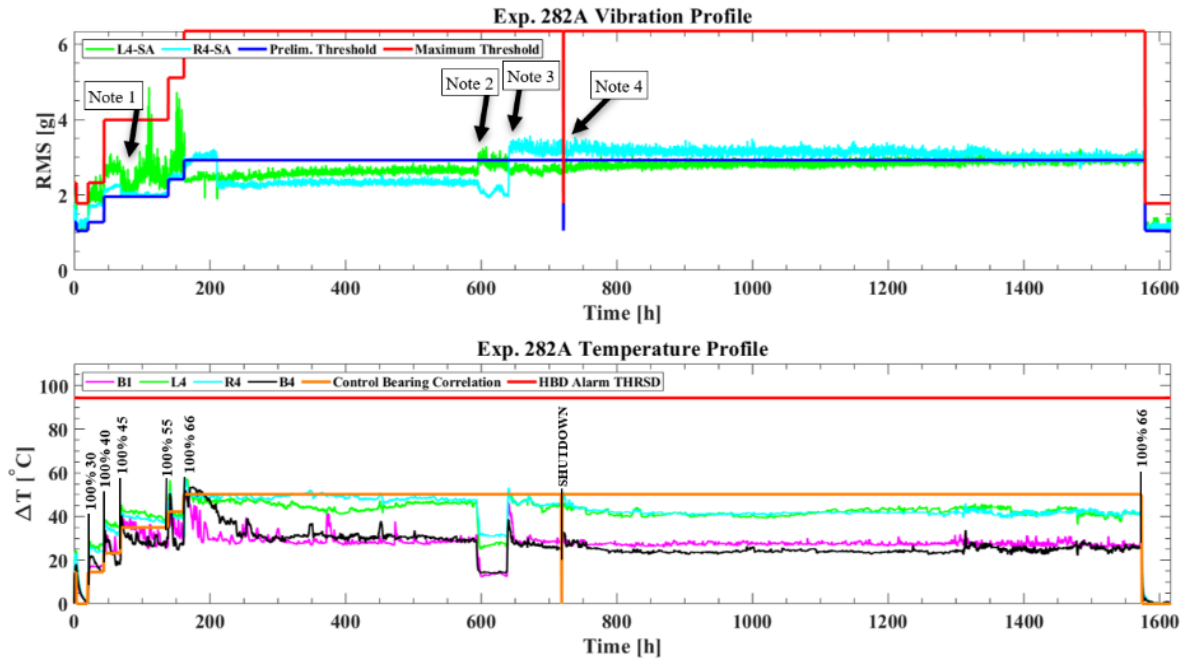


Figure 6: Vibration and temperature above ambient profiles for Exp. 282A

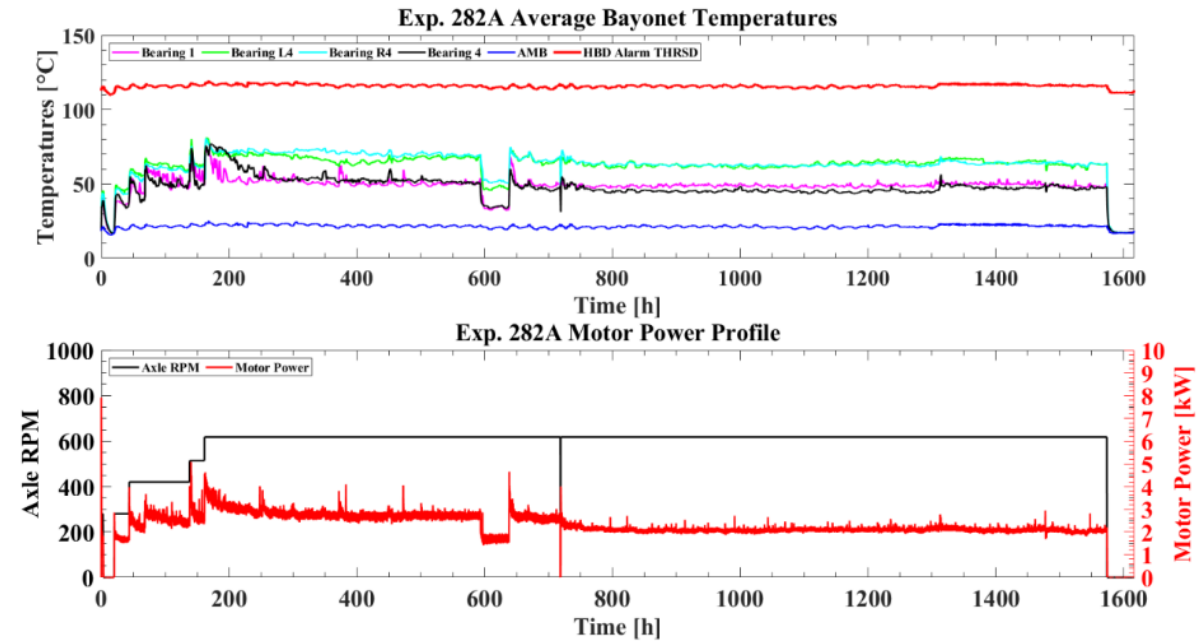


Figure 7: Absolute temperature, motor power, and axle RPM profiles for Exp. 282A

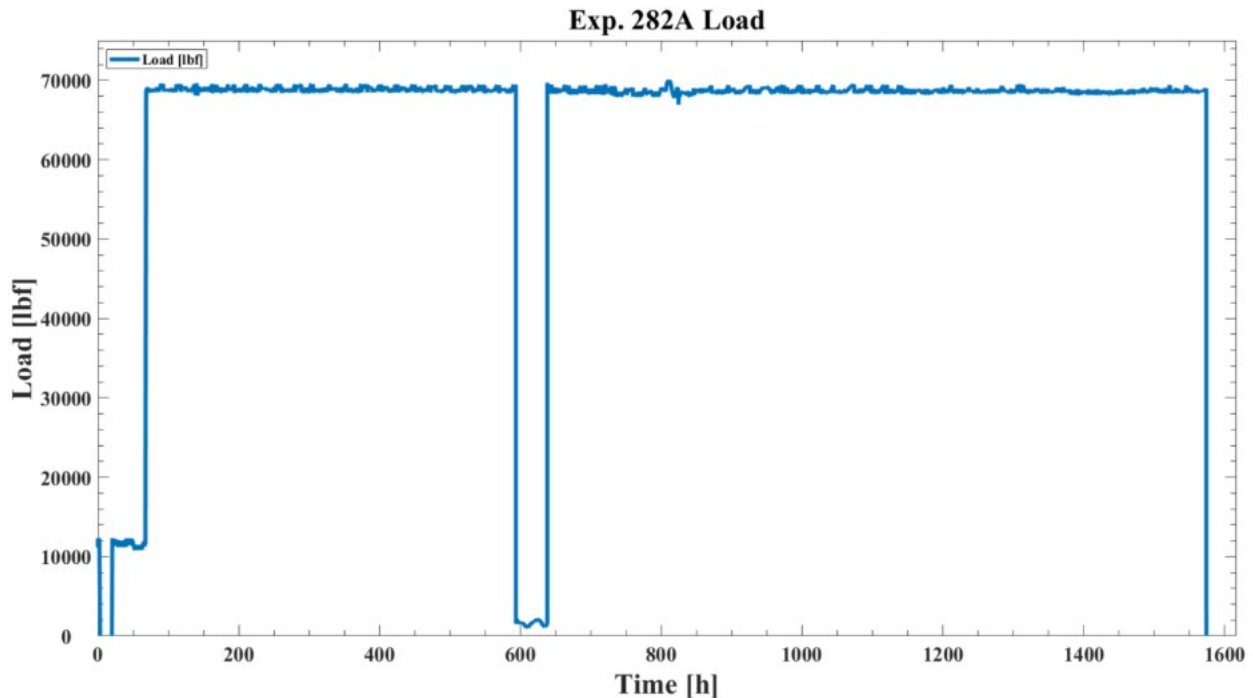


Figure 8: Applied load profile for Exp.282A

**Note 1:** [July 26, 2024] Vibration sensor Y-splitter added as part of a separate concurrent experiment. Instrument was installed between updating file locations; data collection was not affected.

**Note 2:** [August 17, 2024, ~ 11 AM] Load controller anomaly occurred, however it was not caught since it happened on a Saturday morning. Applied load was corrected after 45 hours of low load, at 8 AM Monday, August 19, 2024. Impact of this incident can be seen across all performance profiles.

**Note 3:** [August 19, 2024] Grease was seen beginning to seep out of the inboard (IB) side of L4 in the B2 bearing location and accumulating on the tester table tray.

**Note 4:** [August 22, 2024, ~ 6 PM] A momentary power interruption caused the VFD to shut down, causing the axle to stop rotating. Event was caught within 10 minutes of the VFD shutdown and tester was quickly restarted back to previous operating conditions with no immediate impact.

### 3.1.3 Test Notes

The speed was incrementally increased from 25 mph (40 km/h) to 66 mph (106 km/h) over the course of about 10 days during which the bearings ran for about 21,000 miles (33,800 km), as shown in Figure 6. As a safeguard, initial operating conditions were set to 25 mph at an unloaded railcar condition (i.e., 17% of full load or 5.85 kips per bearing) due to uncertainty regarding the performance of bearings that had remained idle for approximately three years under varying environmental conditions.

The spike in motor power shown in Figure 7 at the start of the test is attributed to the elevated torque required to initiate bearing rotation during the initial start-up. After steady-state operation was achieved,

the operating conditions were adjusted to 45 mph (72 km/h) and 100% load. Detailed test notes are summarized in Table 13. The time in hours (h) is the approximate time the event occurred during this test.

Table 13: Timeline of notable events for Exp. 282A

Notable Events Description	Bearing Location	Mileage [mi]/[km]	Load [%]	Speed [mph]/[km/h]	Time [h]
A vibration sensor Y-splitter was installed as part of a separate concurrent experiment causing a dip in the acceleration. [Note 1] on Figure 6.	N/A	2,129 / 3,427	100	45 / 72	70
Load dropped on Saturday, August 17, 2024, at 11:00 AM. Low load was corrected after 45 hours on Monday, August 19, 2024. [Note 2] on Figure 6.	N/A	35,078 / 56,452	100	66 / 106	595
Grease started seeping out of the inboard (IB) seal of Bearing 2 (L4) on Monday, August 19, 2024. [Note 3] on Figure 6.	Inboard Seal of L4	38,476 / 61,920	100	66 / 106	641
Power outage caused the VFD to shut down. Consequently, the axle stopped rotating. The incident was caught within 10 minutes of its occurrence, and the tester was restarted to its operating conditions prior to the shutdown. [Note 4] on Figure 6.	N / A	40,439 / 65,080	100	66 / 106	721



Figure 9: Pictures showing grease leak from bearing R4



Figure 10: Pictures of grease accumulation below the inboard (IB) seal of bearing L4



Figure 11: Pictures of grease accumulation on IB side of bearing L4

### 3.1.4 Post-Test Teardown and Inspection Pictures

Subsequent to test completion, all four bearings were pressed off the test axle, disassembled, and visually inspected. Photographs were taken before and after cleaning to document the bearing conditions. Selected pictures from the visual inspection are presented hereafter.

#### 3.1.4.1 R4 Bearing – Inboard Cone (Inner Ring)



Figure 12: R4 IB cone raceway



Figure 13: R4 IB cone inner diameter surface

3.1.4.2 R4 Bearing – Outboard Cone (Inner Ring)



Figure 14: R4 outboard (OB) cone raceway



Figure 15: R4 OB cone inner diameter surface

3.1.4.3 *R4 Bearing – Cup (Outer Ring)*

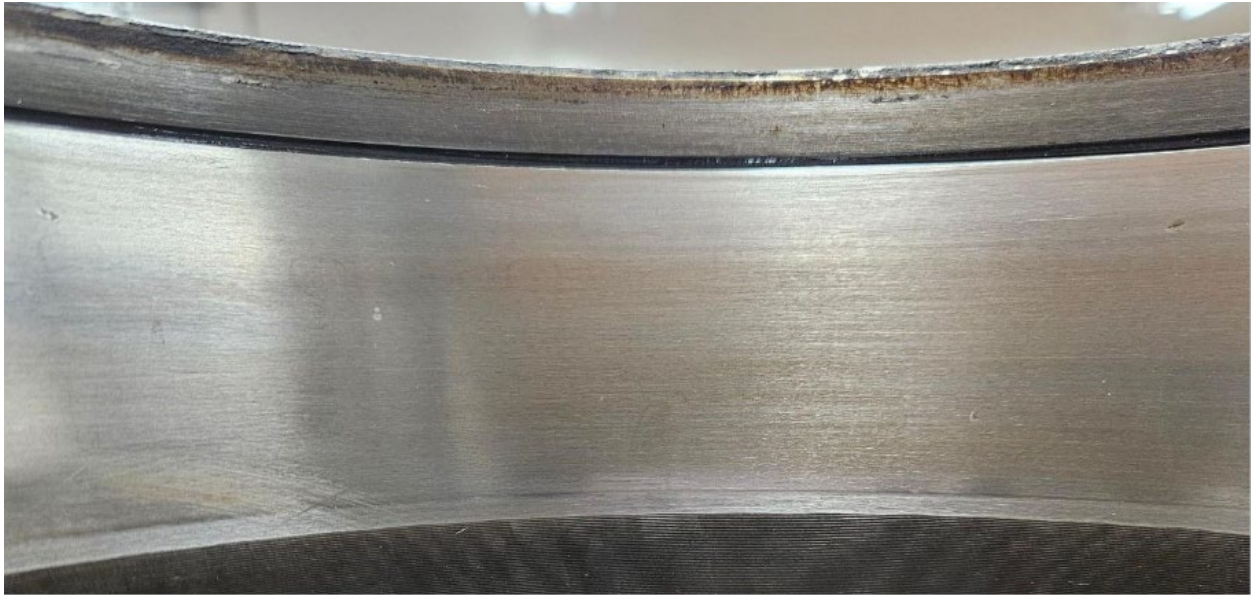


Figure 16: R4 cup OB raceway on loaded side



Figure 17: R4 cup IB raceway on loaded side

3.1.4.4 R4 Bearing – Rollers



Figure 18: R4 IB cone rollers (left) and OB cone rollers (right)

3.1.4.5 L4 Bearing – Inboard Cone (Inner Ring)



Figure 19: L4 IB cone raceway showing repaired spall region

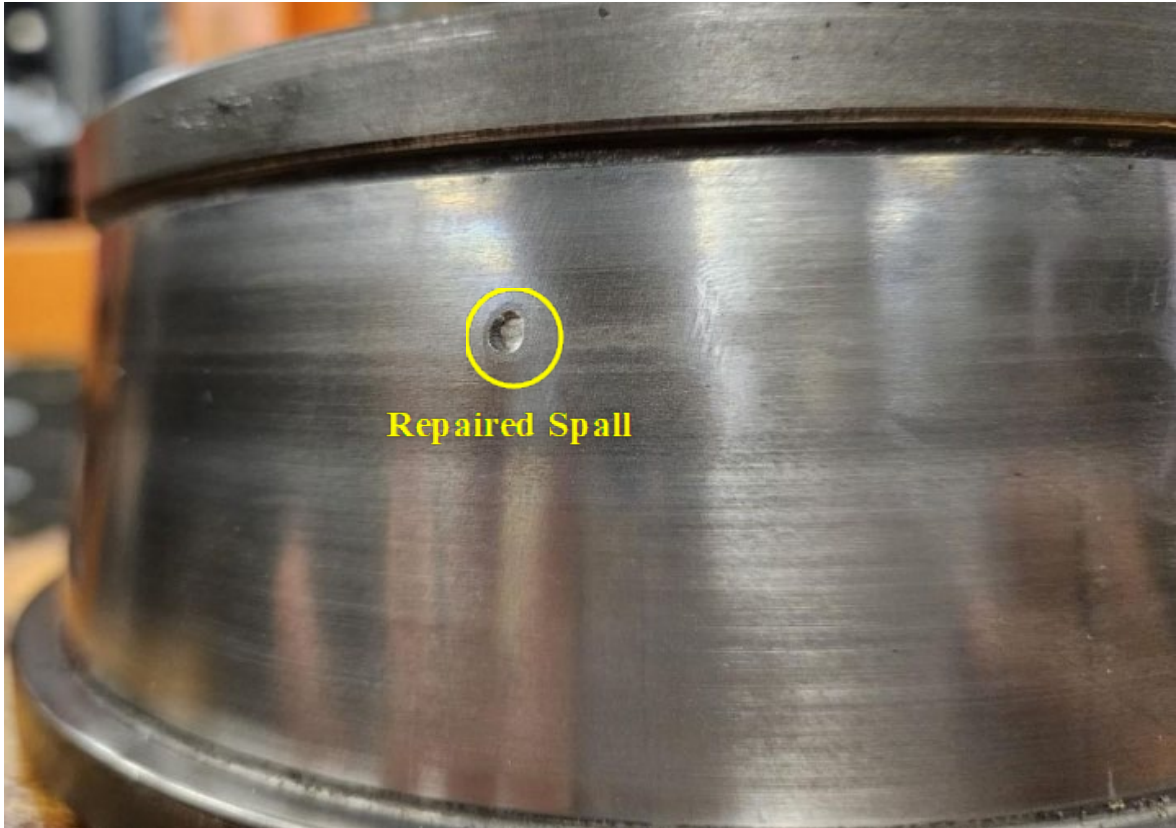


Figure 20: L4 IB cone raceway close-up of repaired spall region



Figure 21: L4 IB cone inner diameter surface

3.1.4.6 *L4 Bearing – Outboard Cone (Inner Ring)*



Figure 22: L4 OB cone raceway



Figure 23: L4 OB cone inner diameter surface

3.1.4.7 L4 Bearing – Cup (Outer Ring)



Figure 24: L4 cup IB raceway on loaded side



Figure 25: L4 cup OB raceway on loaded side

3.1.4.8 *L4 Bearing – Rollers*



Figure 26: L4 IB cone rollers (left) and OB cone rollers (right)

3.1.4.9 *Test Axle Post Press-Off*



Figure 27: Test axle post press-off

### 3.2 Experiment 283A

Experiment 283A ran for a total of 101,461 miles (163,286 kilometers), achieving the target mileage with no evidence of bearing defect initiation. A full teardown and inspection of all four bearings involved in this test were subsequently performed.

#### 3.2.1 Conditions at Shutdown

- Applied Load: **100% load**
- Axle Rotational Speed: **618 RPM**
- Equivalent Train Traveling Velocity: **66 mph (106 km/h)**
- Average Ambient Temperature: **21.7 °C**
- Total Distance Traveled: **101,461 mi (163,286 km)**
- Percentage of 100k Mile Target Distance: **101.5%**
- Average Air Convection Speed Over Bearings: **14.5 mph (23 km/h)**

#### 3.2.2 Data Plots

The vibration and temperature-above-ambient profiles for this experiment are shown in Figure 28. The absolute temperature, motor power, and axle rotational speed profiles are provided in Figure 29, while the applied load profile is plotted in Figure 30.

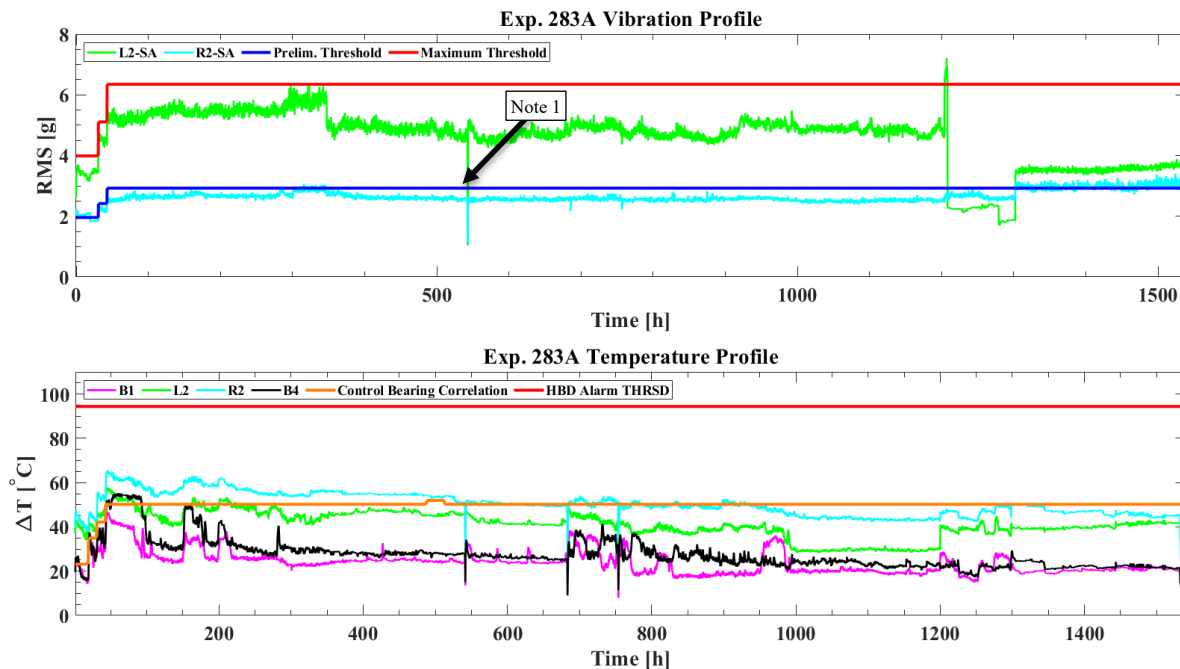


Figure 28: Vibration and temperature above ambient profiles for Exp. 283A

**Note 1:** [November 21, 2024, ~ 3 PM] A momentary power loss activated the tester’s safety features and halted the motor. Event was caught within 20 minutes of the power loss, and the tester was quickly restarted back to previous operating conditions with no immediate impact. Event can be seen across all plots.

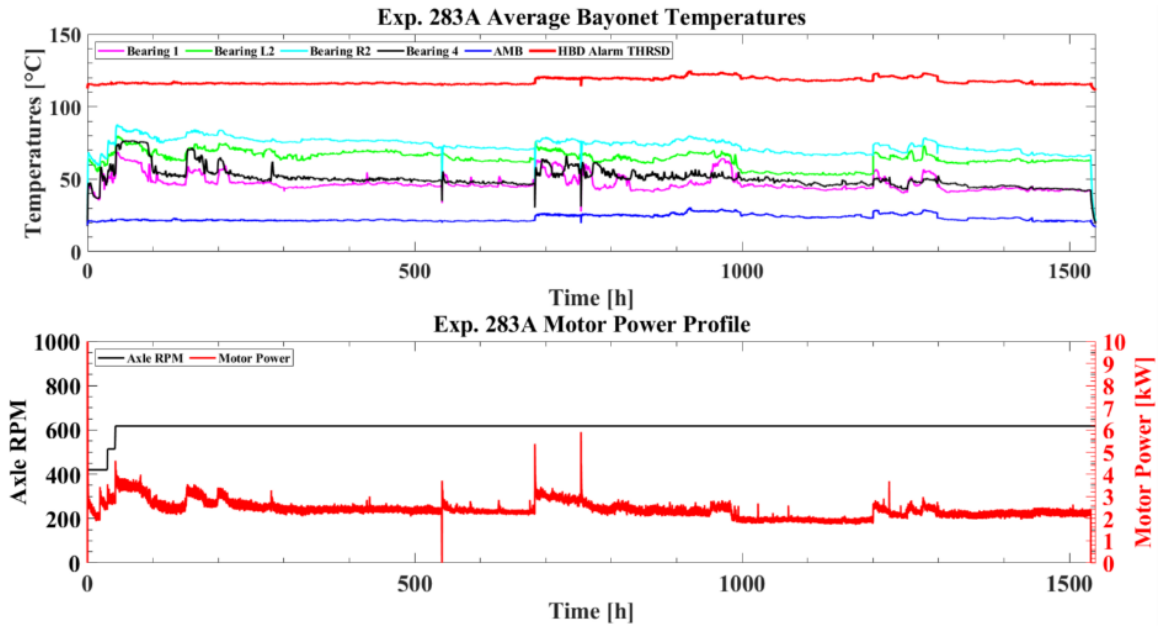


Figure 29: Absolute temperature, motor power, and axle RPM profiles for Exp. 283A

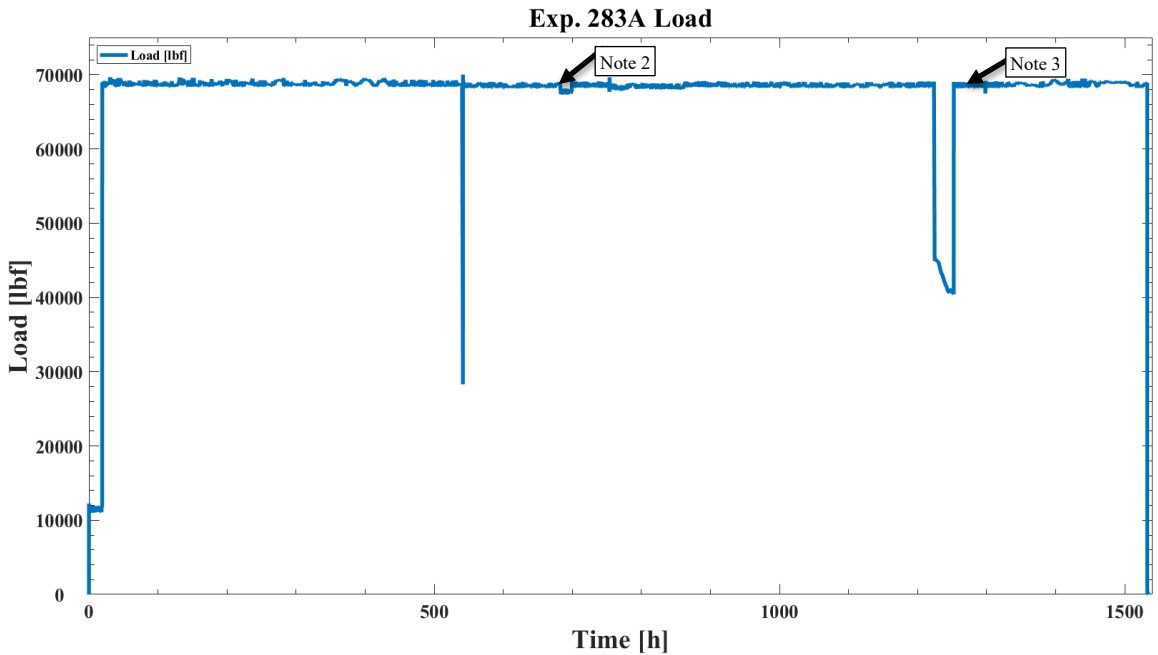


Figure 30: Applied load profile of Exp. 283A

**Note 2:** [December 03, 2024, ~ 8 PM] Load dropped to 67,900 lb<sub>f</sub>. The load was increased to 100% load (68,800 lbf) on December 4, 2024, at 9 AM. Event can be seen across all plots.

**Note 3:** [December 28, 2024, ~ 11 AM] An issue with the load controller occurred while the tester was unmonitored on a Saturday morning. The issue and load were corrected around 2 PM on Sunday, December 29, approximately 27 hours later. Event can be seen across all plots.

### 3.2.3 Test Notes

Figure 28 shows the speed incrementally increased from 45 mph (72 km/h) to 66 mph (106 km/h) over the course of several days, during which the bearings accumulated approximately 2,400 miles (3,862 km) of operation. As a precaution, the operating conditions were initially set to 45 mph (72 km/h) at an unloaded railcar condition. Higher than normal torque was required to initiate rotation at the start of the test runs, as shown in Figure 29. Once steady state operation was achieved, the speed and load were set to 66 mph (106 km/h) and 100% load (full railcar load), respectively. Detailed test notes are summarized in Table 14.

Table 14: Timeline of notable events for Exp. 283A

Notable Events Description	Bearing Location	Mileage [mi]/[km]	Load [%]	Speed [mph]/[km/h]	Time [h]
Tester was started on Monday, October 28, 2024, at 2:30 PM.	N/A	0 / 0	17	45 / 72	0
Grease began to leak out of the inboard seal of Bearing 2 (L2) on Monday, November 05, 2024, depicted in Figure 31.	Inboard Seal of L2	9,791 / 15,758	100	66 / 106	159
Grease began to leak out of the outboard seal of Bearing 3 (R2) on Monday, November 11, 2024, depicted in Figure 33.	Outboard Seal of R2	18,947 / 30,493	100	66/106	297
On Thursday, November 21, 2024, around 3 PM, a momentary power loss activated the tester's safety features and halted the motor. Event was caught within 20 minutes of its occurrence, and the tester was quickly returned to the previous operating conditions with no immediate impact. [Note 1]	N/A	35,174 / 56,608	100	66 / 106	543
The load dropped to 67,900 lbf on December 03, 2024, at 8 PM. The load was re-adjusted to 100% (68,800 lbf) on December 4, 2024, at 9 AM. [Note 2]	N/A	45,676 / 73,509	100	66 / 106	683
An issue with the load controller occurred while the tester was unmonitored on the morning of Saturday, December 28, 2024. The issue and load were corrected around 2 PM on Sunday, December 29, approximately 27 hours later. [Note 3]	N/A	80,789 / 130,017	65	66 / 106	1224
Tester completed mileage goal, and shutdown was initiated on Friday, January 10, 2025.	N/A	101,461 / 163,286	0	0	1540



Figure 31: Grease leaking from the IB seal of Bearing L2 (11/05/2024)



Figure 32: Leaked grease accumulation on IB side of Bearing L2 (11/08/2024)



Figure 33: Grease leaking from OB seal of Bearing R2 (11/11/2024)



Figure 34: Leaked grease accumulation on IB (L2) and OB (R2) sides (11/14/2024)



Figure 35: Leaked grease accumulation on IB side of Bearing L2 (11/18/2024)



Figure 36: Leaked grease accumulation on IB side of Bearing L2 (12/09/2024)

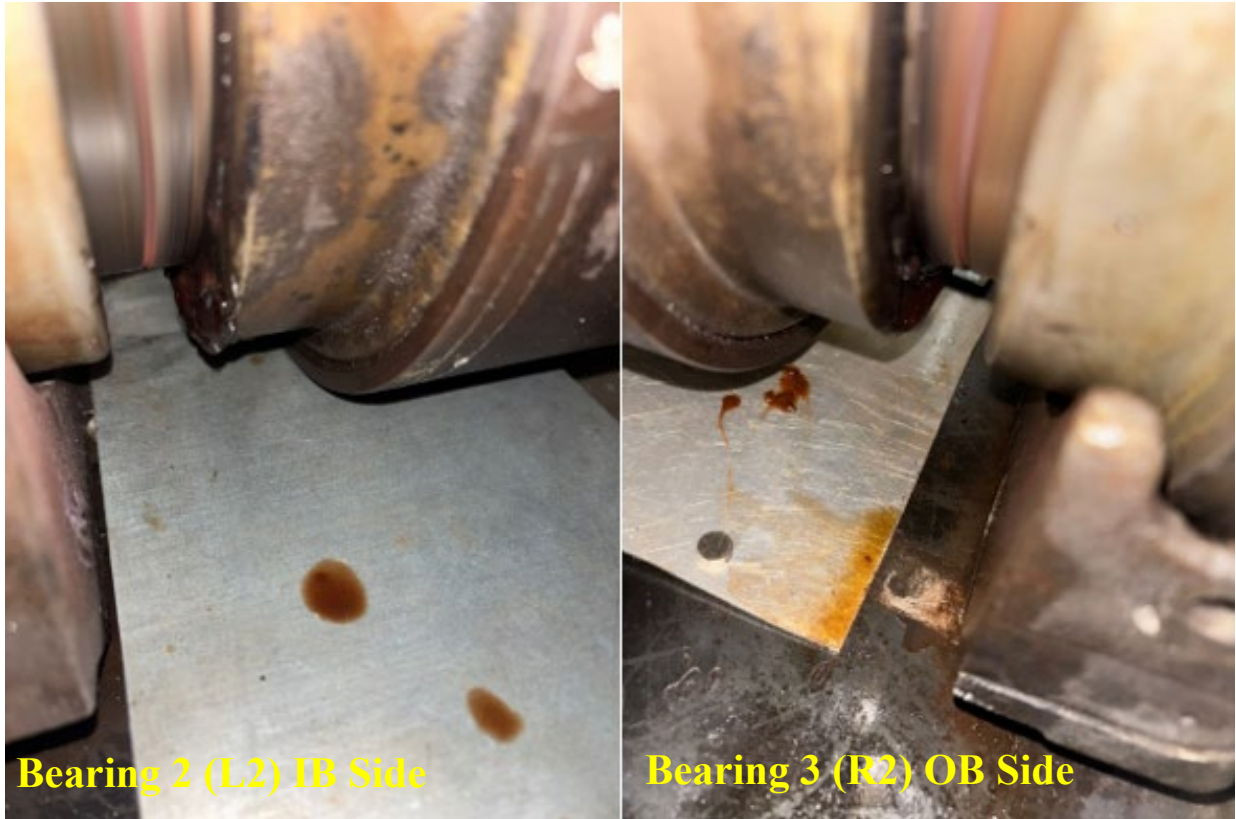


Figure 37: Leaked grease accumulation on IB (L2) and OB (R2) sides (12/17/2024)



Figure 38: Leaked grease accumulation on OB (L2) and IB (R2) sides (12/27/2024)



Figure 39: Leaked grease accumulation on IB (L2) and OB (R2) sides (12/30/2024)



Figure 40: Leaked grease accumulation on IB (L2) and OB (R2) sides (12/31/2024)

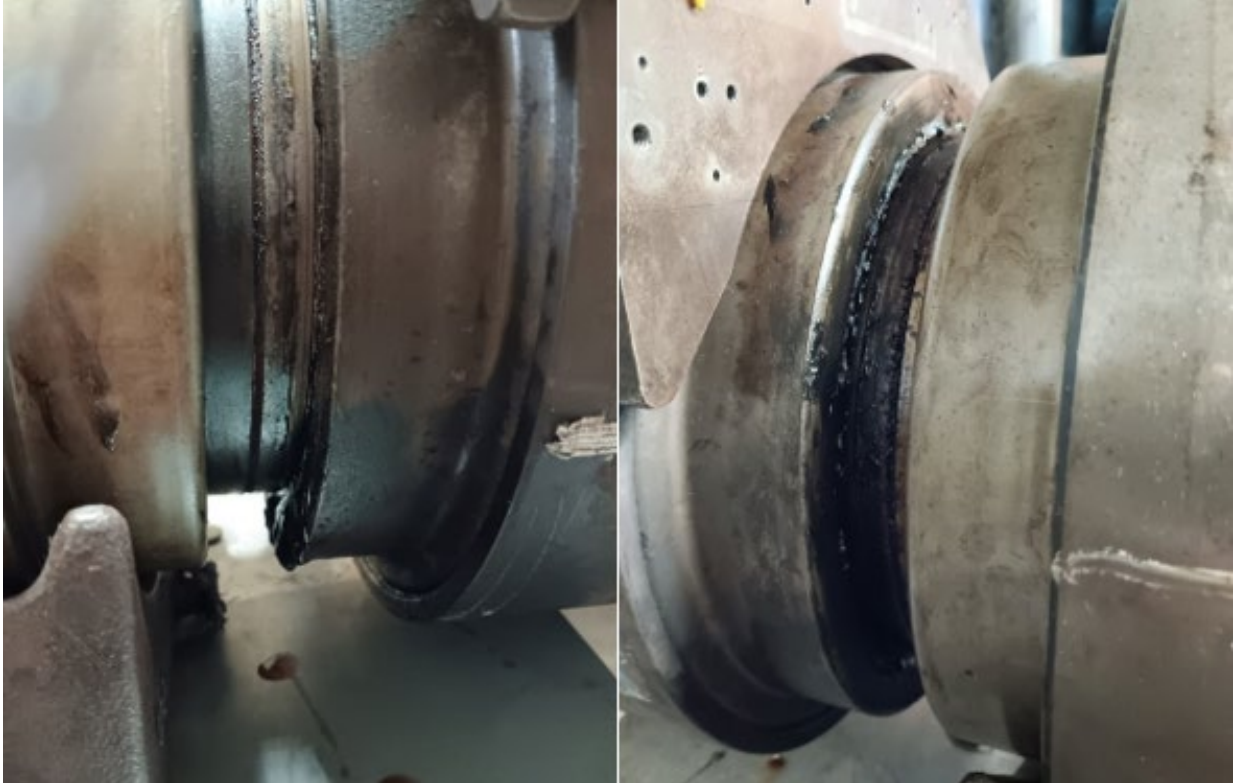


Figure 41: Leaked grease accumulation on IB (L2) and OB (R2) sides (01/02/2025)



Figure 42: Leaked grease accumulation on IB (L2) and OB (R2) sides (01/08/2025)

### 3.2.4 Post-Test Teardown and Inspection Pictures

Subsequent to test completion, all four bearings were pressed off the test axle, disassembled, and visually inspected. Photographs were taken before and after cleaning to document the bearing conditions. Selected pictures from the visual inspection are presented hereafter.

#### 3.2.4.1 R2 Bearing – Inboard Cone (Inner Ring)



Figure 43: R2 IB cone raceway



Figure 44: Small spall (0.015 mm<sup>2</sup> / 0.006 in<sup>2</sup>) on R2 IB cone raceway



Figure 45: Close-up of small spall on R2 IB cone raceway



Figure 46: R2 IB cone inner diameter surface

3.2.4.2 R2 Bearing – Outboard Cone (Inner Ring)



Figure 47: R2 OB cone raceway

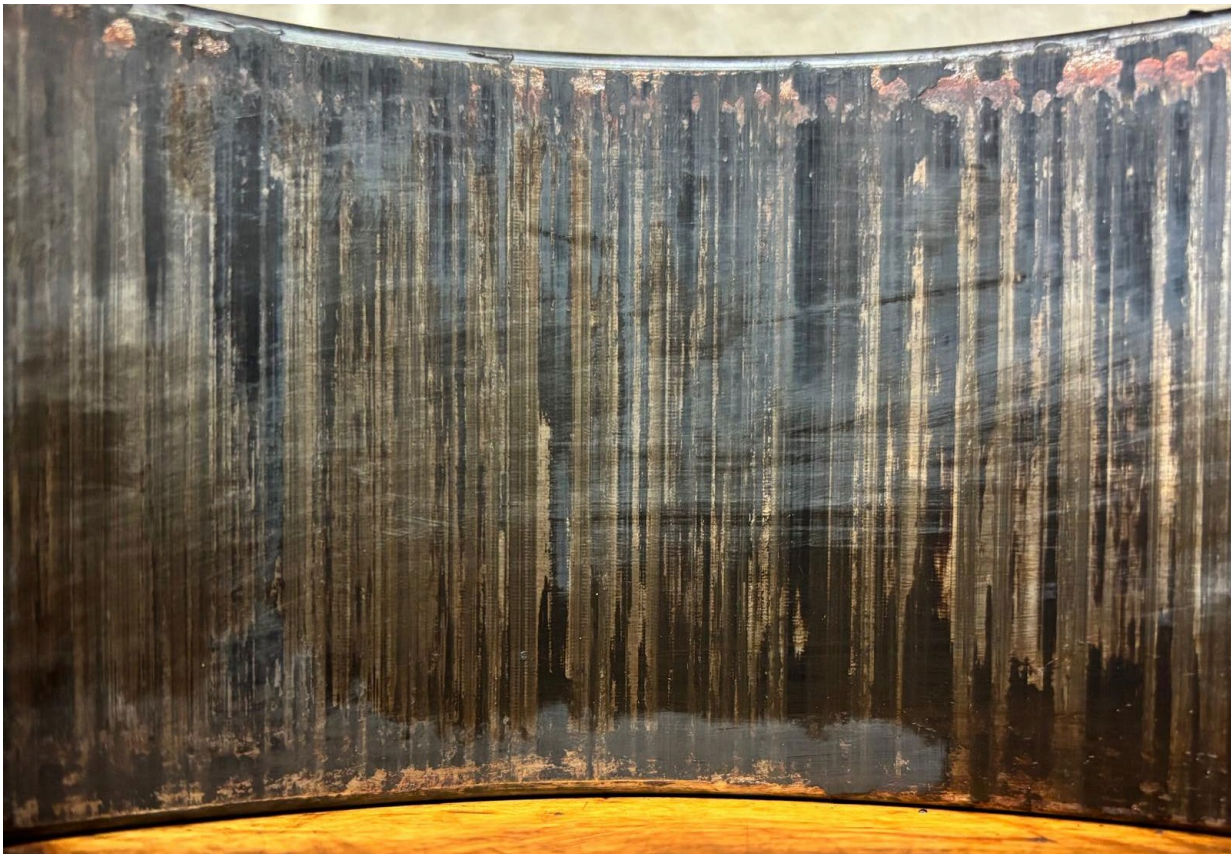


Figure 48: R2 OB cone inner diameter surface

3.2.4.3 R2 Bearing – Cup (Outer Ring)

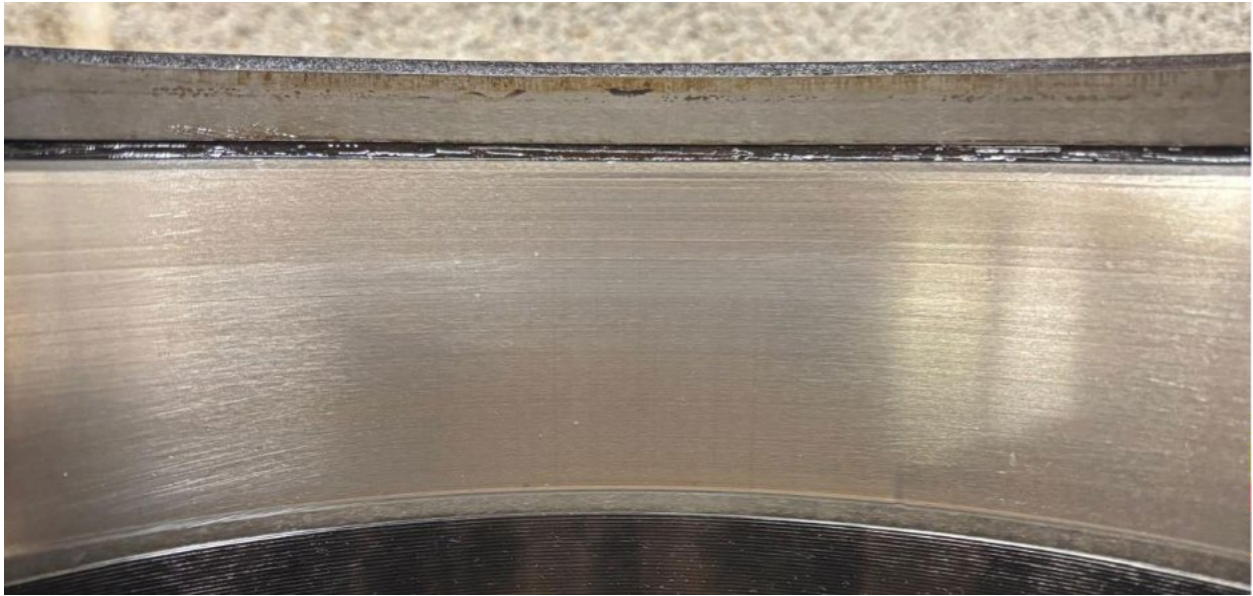


Figure 49: R2 cup OB raceway on loaded side



Figure 50: R2 cup IB raceway on loaded side

3.2.4.4 *R2 Bearing – Rollers*



Figure 51: R2 IB cone rollers (left) and OB cone rollers (right)

3.2.4.5 *L2 Bearing – Inboard Cone (Inner Ring)*



Figure 52: L2 IB cone raceway



Figure 53: L2 IB cone inner diameter surface

3.2.4.6 *L2 Bearing – Outboard Cone (Inner Ring)*



Figure 54: L2 OB cone raceway



Figure 55: L2 OB cone inner diameter surface

3.2.4.7 *L2 Bearing – Cup (Outer Ring)*



Figure 56: L2 cup IB raceway on loaded side



Figure 57: L2 cup OB raceway on loaded side showing a small pit on the raceway

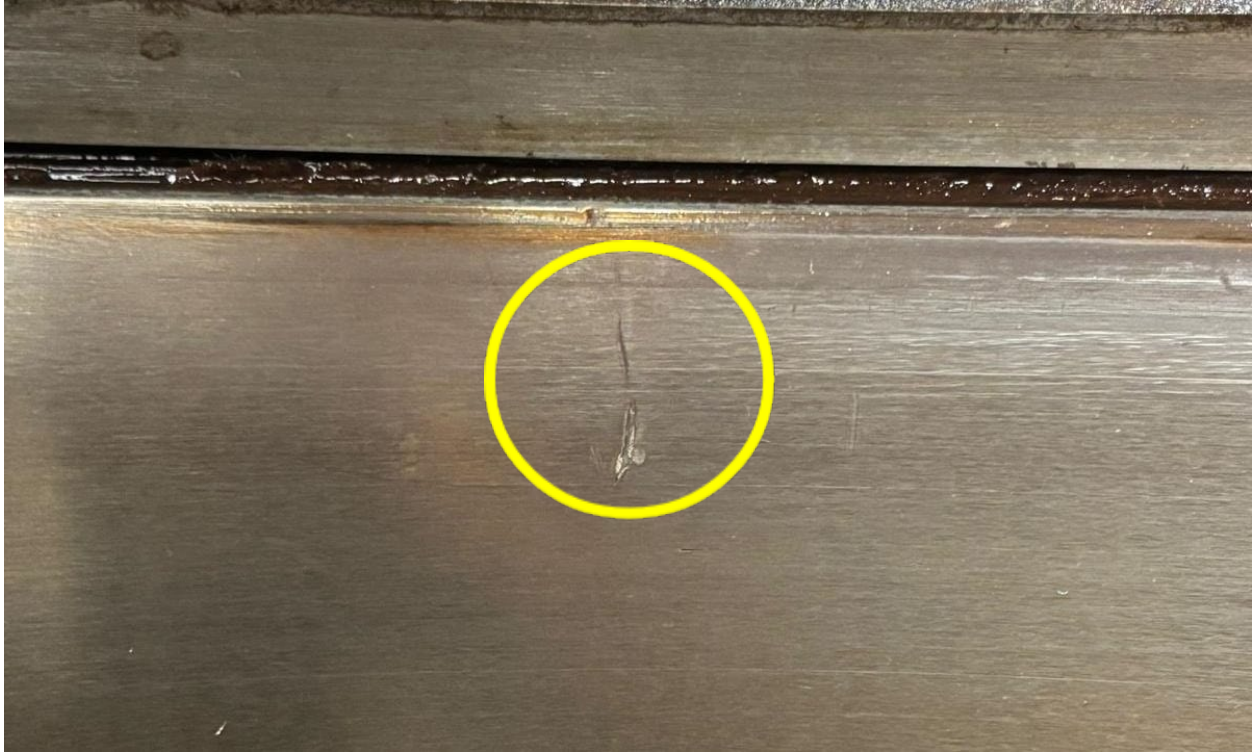


Figure 58: Close-up of minor defect on L2 cup OB raceway on loaded side

#### 3.2.4.8 L2 Bearing – Rollers

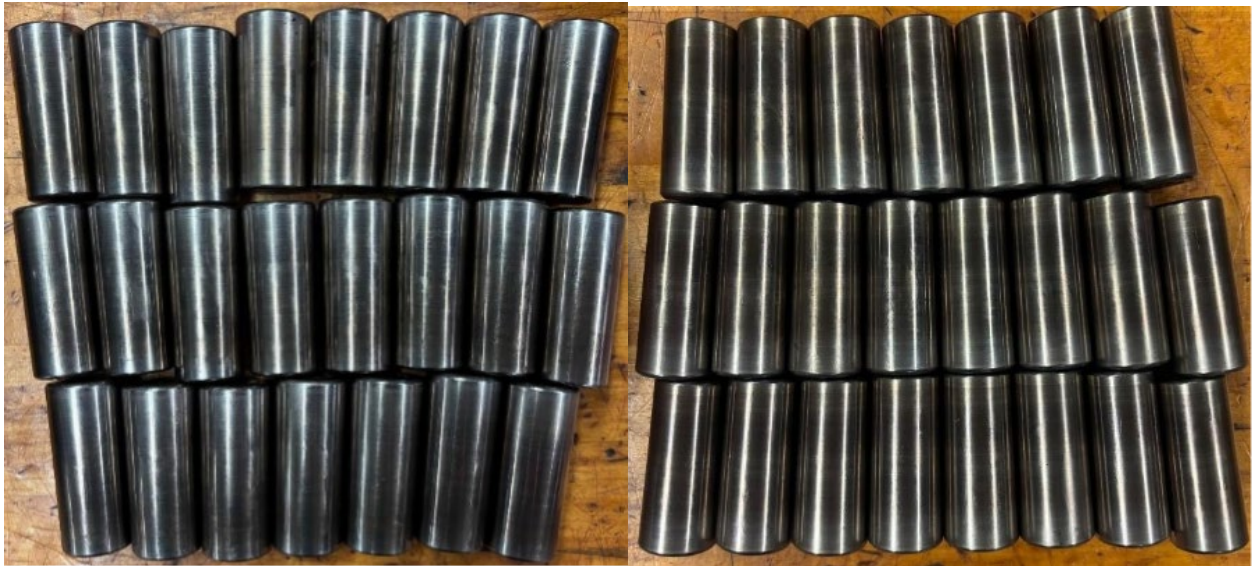


Figure 59: L2 IB cone rollers (left) and OB cone rollers (right)

### 3.2.4.9 Test Axle Post Press-Off



Figure 60: Test axle post press-off

## 3.3 Experiment 304A

Experiment 304A ran for a total of 7,070 miles (11,378 kilometers). Testing was stopped prior to reaching the target mileage after abnormal vibration and temperature readings were observed. A full teardown and inspection of bearing B2 (12-Month inactive bearing) ensued to document its post-test condition.

### 3.3.1 Conditions at Shutdown

- Applied Load: **100% load**
- Axle Rotational Speed: **618 RPM**
- Equivalent Train Traveling Velocity: **66 mph (106 km/h)**
- Average Ambient Temperature: **20 °C**
- Total Distance Traveled: **7,070 mi (11,378 km)**
- Percentage of 100k Mile Target Distance: **7.1%**
- Average Air Convection Speed Over Bearings: **14.5 mph (23 km/h)**

### 3.3.2 Data Plots

The vibration and temperature-above-ambient profiles are provided in Figure 61. The absolute temperature, motor power, and axle rotational speed profiles are provided in Figure 62, while the applied load profile is plotted in Figure 63.

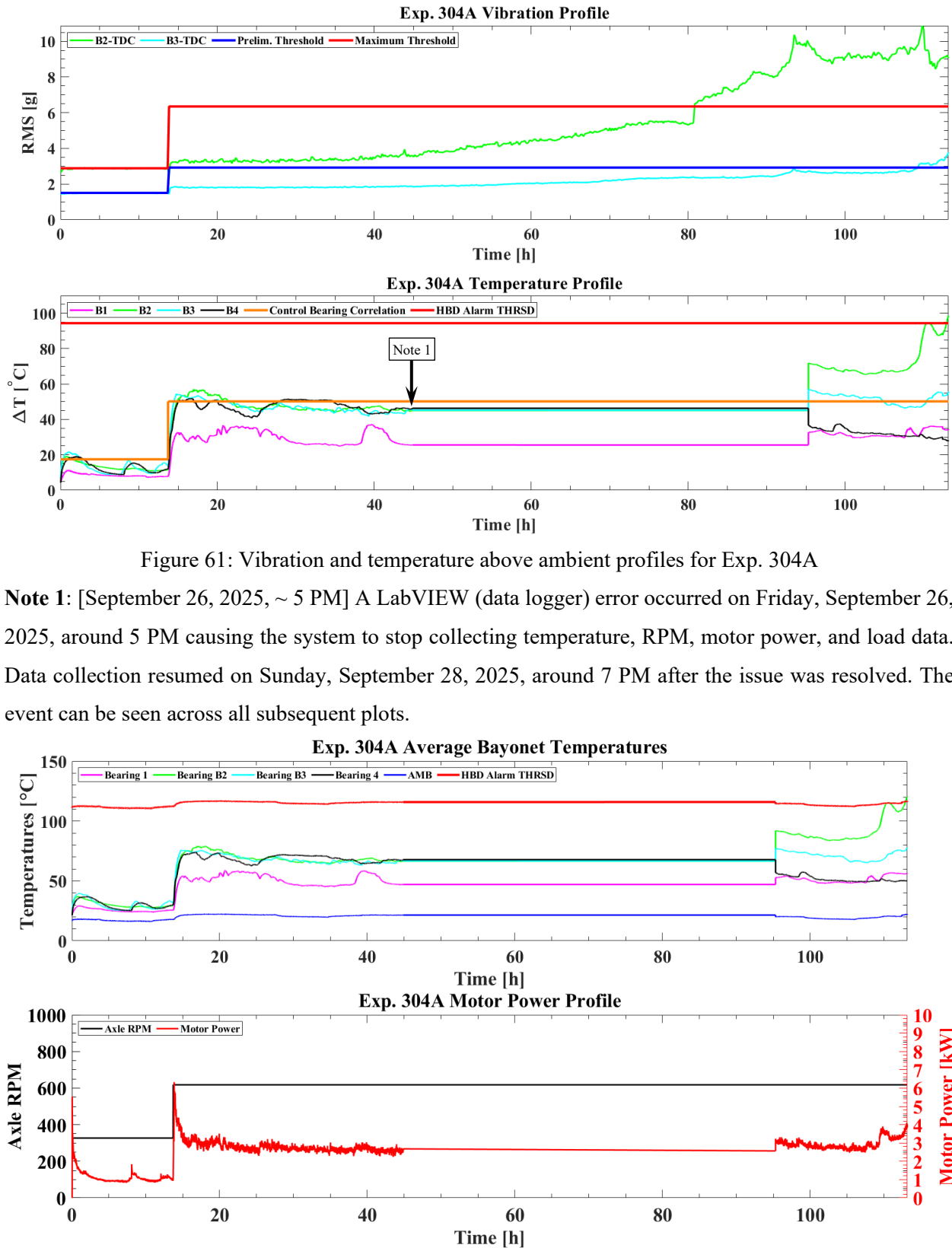


Figure 61: Vibration and temperature above ambient profiles for Exp. 304A

**Note 1:** [September 26, 2025, ~ 5 PM] A LabVIEW (data logger) error occurred on Friday, September 26, 2025, around 5 PM causing the system to stop collecting temperature, RPM, motor power, and load data. Data collection resumed on Sunday, September 28, 2025, around 7 PM after the issue was resolved. The event can be seen across all subsequent plots.

Figure 62: Absolute temperature, motor power, and axle RPM profiles for Exp. 304A

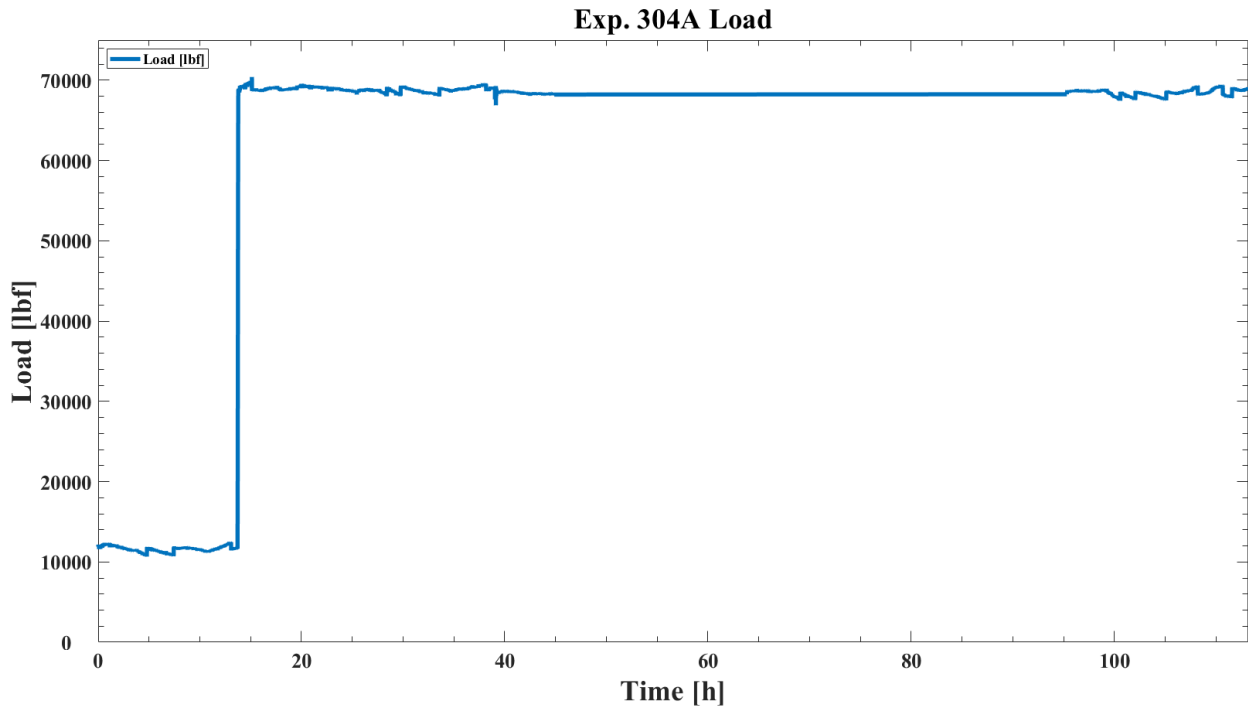


Figure 63: Applied load profile for Exp. 304A

### 3.3.3 Test Notes

Figure 61 shows the increase in speed from 35 mph (56 km/h) to 66 mph (106 km/h) as the applied load was raised from 17% (i.e., empty railcar load) to 100% (i.e., fully loaded railcar) of the AAR suggested load rating for class F and K bearings. The test began under an unloaded railcar condition (17% load) and was transitioned to 66 mph (106 km/h) speed and 100% load condition once steady-state operation was achieved. However, the test was terminated early after only 7,070 miles (11,378 kilometers) of operation because the vibration levels within the 12-Month bearing increased beyond the maximum threshold indicating that a defect has developed, and the bearing operating temperature exceeded the AAR hot bearing detector alarm threshold of 94.4°C (170°F) above ambient. Detailed test notes are summarized in Table 15.

The vibration data collected from the experiment was analyzed using the Level 2 vibration analysis developed by the researchers at the UTCRS [3]. Examining Table 16, the Level 2 analysis indicated the presence of both cup and cone spalls on the raceways of the bearing. A full teardown and visual inspection of bearing B2 (12-Month bearing) was performed based on the vibration and temperature profiles of this bearing.

Table 15: Timeline of notable events for Exp. 304A

Notable Events Description	Bearing Location	Mileage [mi]/[km]	Load [%]	Speed [mph]/[km/h]	Time [h]
Tester started on Wednesday, September 24, 2025, at 7:00 PM.	N/A	0 / 0	17	35 / 56	0
Speed and load increased to 66 mph (106 km/h) and full load operating conditions on Thursday, September 25, 2025, at 9:00 AM.	N/A	584 / 940	100	66 / 106	15
LabVIEW (data logger) error occurred on Friday, September 26, 2025, at 5:00 PM, causing the system to stop collecting temperature, motor power, RPM, and load data. Data collection resumed on Sunday at 7:00 PM after the issue was resolved. [Note 1]	N/A	5,879 / 9,461	100	66 / 106	44.5
Tester was stopped on Monday, September 29, 2025, at 4:00 PM after abnormal noise, elevated temperature, and high RMS vibration levels were observed. The bearing operating temperature exceeded the AAR hot bearing detector alarm threshold of 94.4°C (170°F) above ambient.	B2	7,070 / 11,378	100	66 / 106	113.2

Table 16: Bearing B2 Level 2 vibration analysis [3]

Level 2 Analysis				
	Folder	18	19	20
	Speed [RPM/MPH]	618/66	618/66	618/66
B2 – 12 Month	Certainty [%]	<b>88.88</b>	<b>87.30</b>	<b>95.24</b>
	Defective Component	Cone	Cup	Cup

### 3.3.4 Post-Test Teardown and Inspection Pictures

After the test was terminated, bearings B1 and B2 (12-Month) were pressed off the test axle, disassembled, and visually inspected. Pictures were taken before and after cleaning the bearings to document their post-test condition. Since only B1 and B2 were removed to allow continued testing, a post press-off image of the full test axle is not included for this experiment. The images from the visual inspection performed are presented in the following subsections.

3.3.4.1 B2 (12-Month) Bearing – Inboard Cone (Inner Ring)



Figure 64: B2 (12-Month) bearing IB cone raceway



Figure 65: B2 (12-Month) bearing IB cone inner diameter surface

3.3.4.2 B2 (12-Month) Bearing – Outboard Cone (Inner Ring)



Figure 66: B2 (12-Month) bearing OB cone raceway – Picture 1



Figure 67: B2 (12-Month) bearing OB cone raceway – Picture 2



Figure 68: B2 (12-Month) bearing OB cone raceway – Picture 3



Figure 69: B2 (12-Month) bearing OB cone raceway – Picture 4



Figure 70: B2 (12-Month) bearing OB cone inner diameter surface

#### 3.3.4.3 B2 (12-Month) Bearing – Cup (Outer Ring)

All photographs were taken using a consistent orientation reference system to document the raceway condition of the cup. The orientation is defined by viewing the test axle from the end-cap side, as illustrated in Figure 71. In this convention,  $0^\circ$  corresponds to the fan side (right),  $90^\circ$  represents the loaded side (top),  $180^\circ$  indicates the non-fan side (left), and  $270^\circ$  represents the unloaded side (bottom). The loaded side ( $90^\circ$ ) corresponds to the region where the hydraulic cylinder applies direct load during testing.

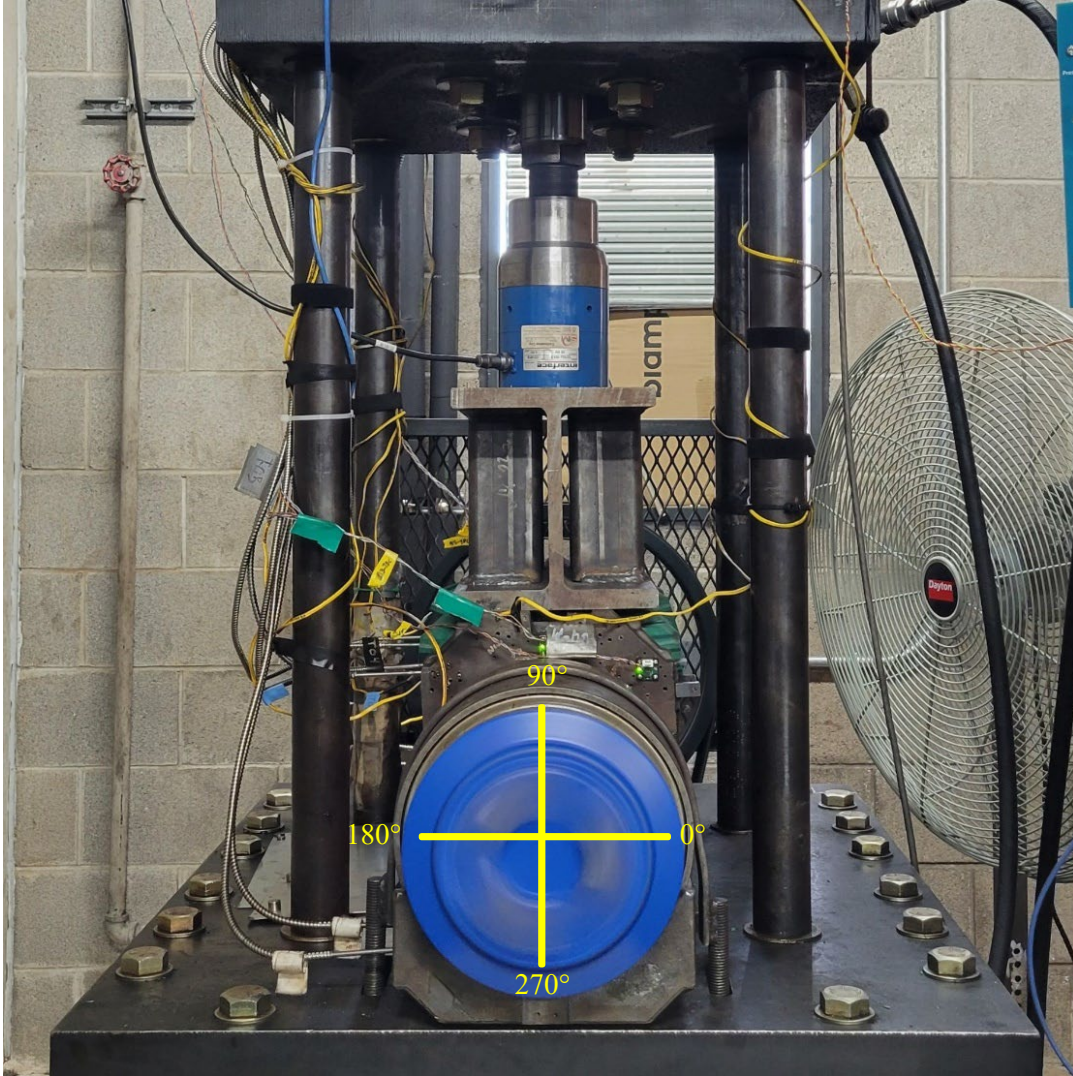


Figure 71: Orientation convention for cup documentation (view from end-cap side of the test axle)

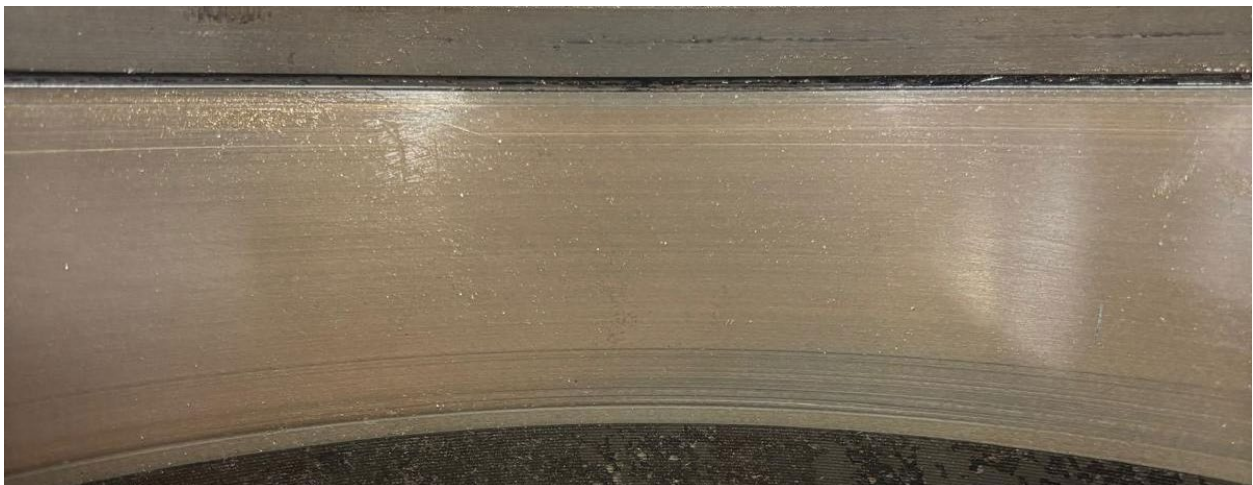


Figure 72: B2 (12-Month) bearing cup IB raceway on fan side (0°)



Figure 73: B2 (12-Month) bearing cup IB raceway on loaded side (90°)

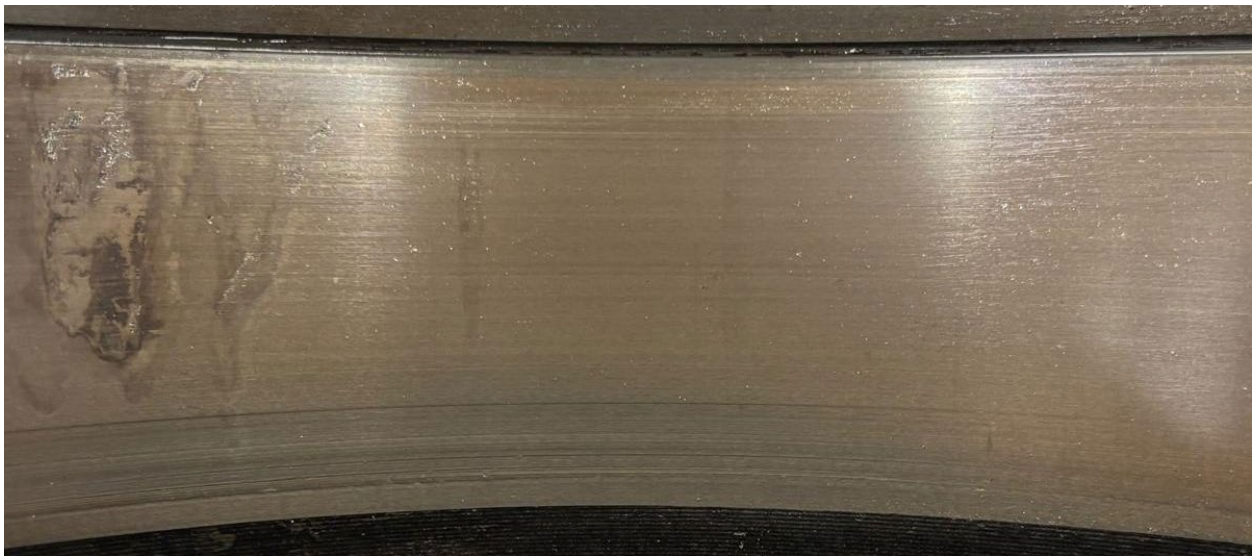


Figure 74: B2 (12-Month) bearing cup IB raceway on non-fan side (180°)



Figure 75: B2 (12-Month) bearing cup IB raceway on unloaded side (270°)



Figure 76: B2 (12-Month) bearing cup OB raceway on fan side (0°)



Figure 77: B2 (12-Month) bearing cup OB raceway on loaded side (90°)



Figure 78 : B2 (12-Month) bearing cup OB raceway on non-fan side (180°)



Figure 79: B2 (12-Month) bearing cup OB raceway on unloaded side (270°)

#### 3.3.4.4 B2 (12-Month) Bearing – Rollers



Figure 80: B2 (12-Month) bearing IB cone rollers (left) and OB cone rollers (right)

#### 3.3.5 Spall Analysis

Visual inspection indicated that most severe damage was concentrated on the outboard-side components of the 12-Month bearing, including the cone and cup raceways as well as several rollers. The outboard cone and cup surfaces exhibited a brown heat tint, likely associated with elevated operating temperatures during testing, which reached approximately 98.5°C (177°F) above ambient. In contrast, the inboard components displayed minor surface distress, with several small spalls observed on the inboard side of the cup. All

observed damage was systematically documented for each affected component, followed by detailed spall area measurements to quantify the extent of surface degradation.

Spall area measurements were obtained by creating multiple imprints of the major damaged regions using molten bismuth. Each imprint was subsequently scanned and processed using image-analysis software to determine the spall area and the corresponding percentage of the total surface area. Multiple spalls were also identified on the roller surfaces and were documented and analyzed using the same image-processing software. The spall mapping process is presented in detail in reference [2].



Figure 81: B2 (12-Month) bearing OB cup spall with an area of 4.57 in<sup>2</sup> (29.48 cm<sup>2</sup>) (left) and 7.31 in<sup>2</sup> (47.16 cm<sup>2</sup>) (right)



Figure 82: B2 (12-Month) bearing OB cone spall with an area of 3.18 in<sup>2</sup> (20.52 cm<sup>2</sup>) (left) and 3.32 in<sup>2</sup> (21.42 cm<sup>2</sup>) (right)



Figure 83: B2 (12-Month) bearing OB cone spall with an area of 3.12 in<sup>2</sup> (20.13 cm<sup>2</sup>) (left) and 3.96 in<sup>2</sup> (25.55 cm<sup>2</sup>) (right)



Figure 84: B2 (12-Month) bearing OB cone spall with an area of 4.41 in<sup>2</sup> (28.45 cm<sup>2</sup>) (left) and 4.27 in<sup>2</sup> (27.55 cm<sup>2</sup>) (right)



Figure 85: B2 (12-Month) bearing OB cone spall with an area of 2.03 in<sup>2</sup> (13.10 cm<sup>2</sup>) (left) and 0.42 in<sup>2</sup> (2.71 cm<sup>2</sup>) (right)

A summary of the spall area measurements is provided in Table 17. The outboard cone exhibited the most significant damage, with approximately 58% of the total cone raceway area affected by spalling. The outboard cup also showed significant degradation, with roughly 22% of its raceway area damaged. In contrast, the inboard cup exhibited only minor surface damage, representing about 1% of its total raceway area. Spalling was present on all rollers of the outboard cone assembly to varying degrees of severity and collectively accounted for approximately 11% of the total roller surface area for that cone assembly. Figure 86 shows five of the most severe roller spalls.



Figure 86: B2 (12-Month) bearing OB cone assembly roller spalls with areas of 1.30 in<sup>2</sup> (8.39 cm<sup>2</sup>), 1.45 in<sup>2</sup> (9.35 cm<sup>2</sup>), 2.41 in<sup>2</sup> (15.55 cm<sup>2</sup>), 0.84 in<sup>2</sup> (5.42 cm<sup>2</sup>), and 1.07 in<sup>2</sup> (6.90 cm<sup>2</sup>) [left to right]

Table 17: B2 (12-Month) bearing spall (damage) area measurements

Damaged Area	Spall (Damage) Size [in <sup>2</sup> ]	Total Raceway Area [in <sup>2</sup> ]	Percentage of Area Spalled [%]
Outboard Cone	25.06	43.26	58
Inboard Cup	0.60	56.93	1
Outboard Cup	12.32	56.93	22
Outboard Cone Rollers	12.98	114.77	11
<b>Bearing – Total</b>	<b>50.96</b>	<b>429.92*</b>	<b>12</b>

\*Total bearing raceway surface area for 2 cones, 2 cups, and 46 rollers.

Overall, the total damaged area within the 12-Month bearing was estimated to be 50.96 in<sup>2</sup> (328.77 cm<sup>2</sup>), representing approximately 25% of the combined 200.38 in<sup>2</sup> total raceway surface area for all four raceways in an AAR class F bearing. It is important to note that the severe damage observed on the 12-Month inactive bearing was accurately depicted by the acquired vibration and temperature signatures of that bearing during testing, and reflected in the Level 2 analysis results summarized in Table 16. Moreover, Figure 61 demonstrates how the vibration signature captures the onset of spall initiation as the vibration levels begin to slowly trend upwards indicating the propagation of the spall under the operating conditions.

### 3.4 Experiment 304B

Experiment 304B was initiated following the removal of bearing B2 (12-Month) after completion of Experiment 304A. A healthy, defect-free bearing was installed in its position to allow continued evaluation of the bearing subjected to approximately six months of outdoor environmental exposure.

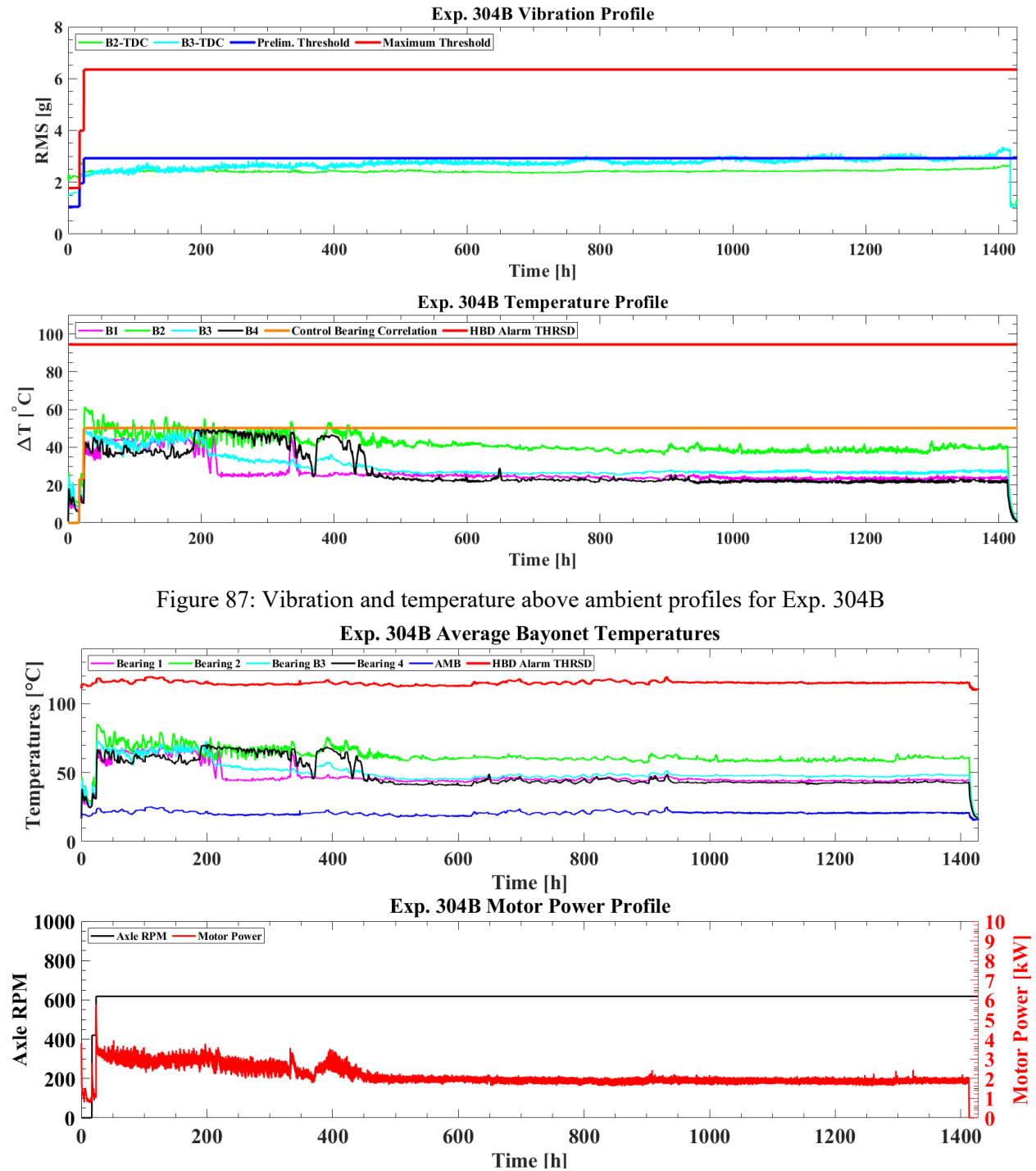
Bearing B3 (6-Month inactive bearing) ran for a total of 100,014 miles (160,957 kilometers), achieving the target mileage with no evidence of bearing defect initiation. This mileage represents the cumulative distance traveled by bearing B3 across Experiments 304A (7,070 miles) and 304B (92,944 miles). A full teardown and inspection of all four bearings involved in this test was subsequently performed.

#### 3.4.1 Conditions at Shutdown

- Applied Load: **100% load**
- Axle Rotational Speed: **618 RPM**
- Equivalent Train Traveling Velocity: **66 mph (106 km/h)**
- Average Ambient Temperature: **21.0 °C**
- Total Distance Traveled: **100,014 mi (160,957 km)**
- Percentage of 100k Mile Target Distance: **100.01%**
- Average Air Convection Speed Over Bearings: **14.5 mph (23 km/h)**

### 3.4.2 Data Plots

The vibration and temperature-above-ambient profiles for this experiment are shown in Figure 87. The absolute temperature, motor power, and axle rotational speed profiles are provided in Figure 88, and the applied load profile is plotted in Figure 89.



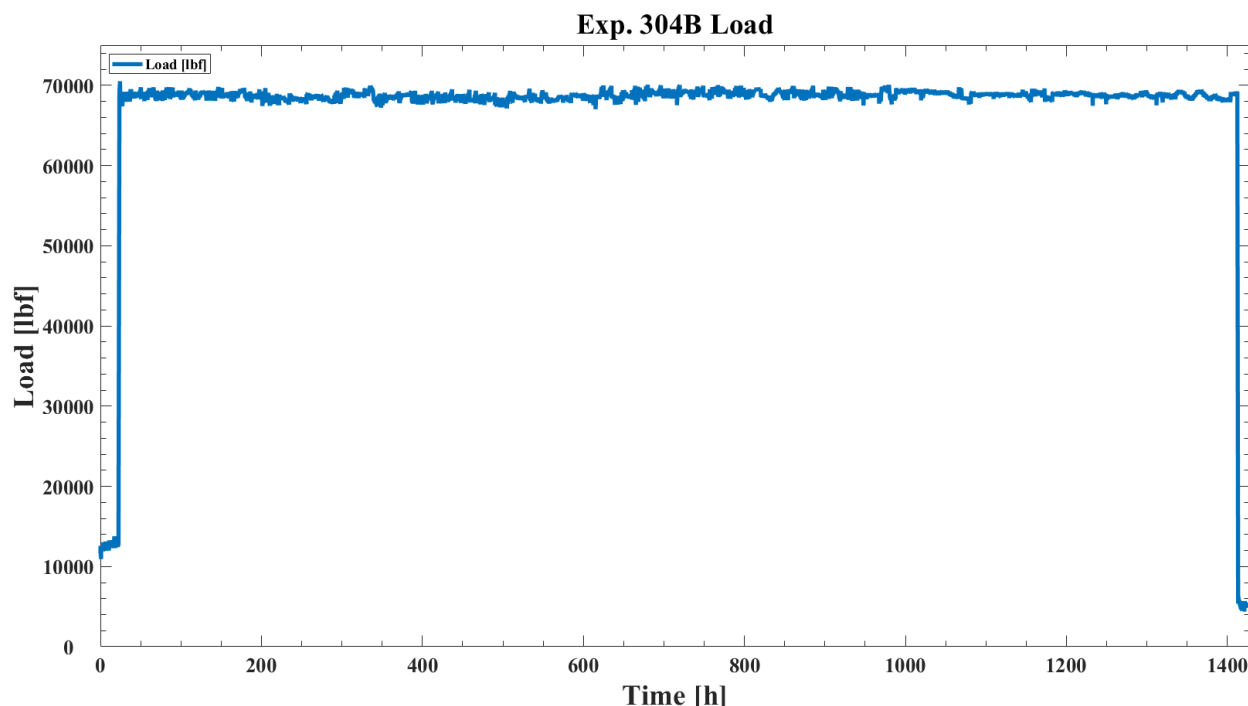


Figure 89: Applied load profile for Exp. 304B

### 3.4.3 Test Notes

The speed was incrementally increased from 25 mph (40 km/h) to 66 mph (106 km/h) as the applied load was raised from 17% to 100% of the full AAR load rating for a class F bearing, as shown in Figure 88. Detailed test notes are summarized in Table 18.

Table 18: Timeline of notable events for Exp. 304B

Notable Events Description	Bearing Location	Mileage [mi]/[km]	Load [%]	Speed [mph]/[km/h]	Time [h]
Tester started on Monday, October 13, 2025, at 11:00 AM.	N/A	0 / 0	17	25 / 40	0
Speed and load increased to 66 mph (106 km/h) and full load operating conditions on Tuesday, October 14, 2025, at 5:00 PM.	N/A	751 / 1,209	100	66 / 106	30
Bearing B3 (6-Month inactive bearing) completes milage goal, and shut down was initiated on Tuesday, December 16, 2025, at 6:00 PM.	N/A	92,944 / 149,579	100	66 / 106	1,413

### 3.4.4 Post-Test Teardown and Inspection Pictures

Following completion of Experiment 304B, all four bearings were removed from the test axle, disassembled, and visually inspected. Photographs were obtained before and after cleaning to document their post-test condition. Selected images from the inspection are presented in the following subsections.

3.4.4.1 B3 (6-Month) Bearing – Inboard Cone (Inner Ring)



Figure 90: B3 (6-Month) bearing IB cone raceway



Figure 91: B3 (6-Month) bearing IB cone inner diameter surface

3.4.4.2 B3 (6-Month) Bearing – Outboard Cone (Inner Ring)



Figure 92: B3 (6-Month) bearing OB cone raceway



Figure 93: B3 (6-Month) bearing OB cone inner diameter surface

3.4.4.3 B3 (6-Month) Bearing – Cup (Outer Ring)



Figure 94: B3 (6-Month) bearing cup OB raceway on loaded side

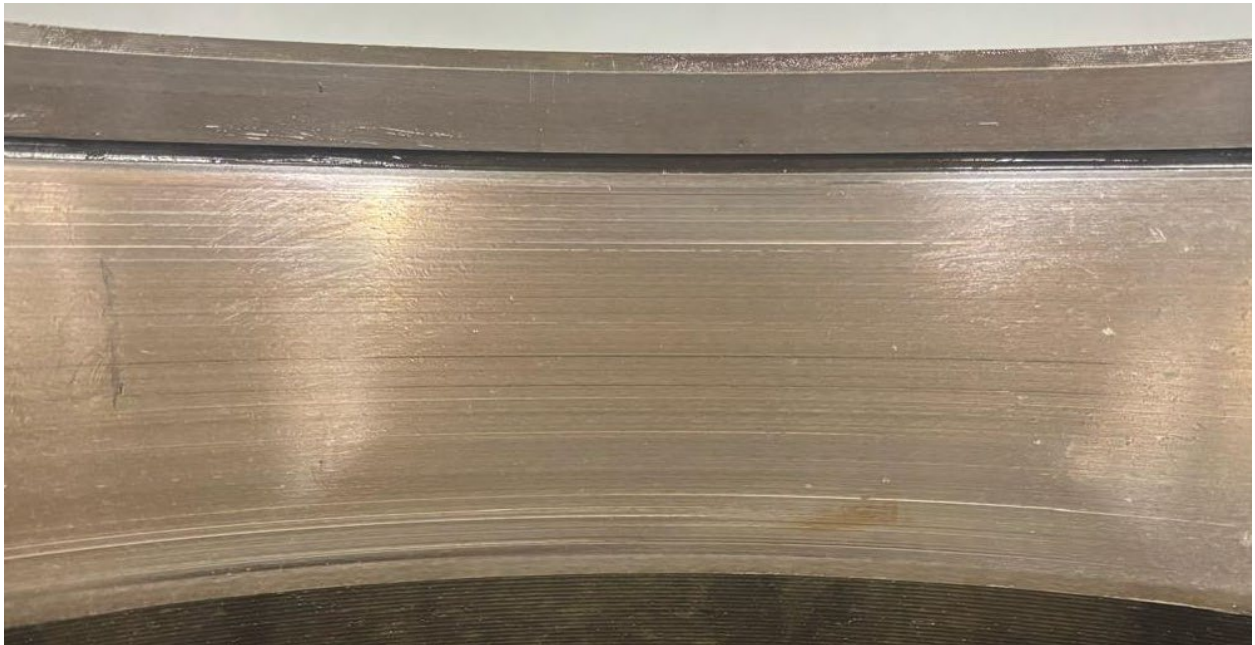


Figure 95: B3 (6-Month) bearing cup IB raceway on loaded side

3.4.4.4 B3 (6-Month) Bearing – Rollers



Figure 96: B3 (6-Month) IB cone rollers (left) and OB cone rollers (right)

3.4.4.5 Test Axle Post-Press-Off



Figure 97: Test axle post-press-off

## 4 Test Observations

Bearing condition was monitored routinely during the experiments, and all abnormal operating conditions were recorded. Unsupervised operation of the test rig (overnight or during weekends) was suspended when the bearings were assessed to be at risk of imminent failure.

### 4.1 Experiment 282A

As the test progressed, grease leakage was observed from the inboard side of bearing L4 over a period of several weeks, as can be seen in Figure 10 and Figure 11. Aluminum plates and tarps were installed to capture the released grease and facilitate subsequent collection and analysis.

Figure 6 and Figure 7 show that the operating temperatures of the two inactive bearings (R4 and L4) were comparable throughout the test and were approximately 15°C (27°F) higher than the two control bearings on the same test axle. However, it should be noted that the operating temperatures of both inactive bearings were within the range of average operating temperatures of healthy bearings at the same speed and load conditions, and well below the 94.4°C (170°F) above ambient recommended AAR alarm threshold for Hot Bearing Detectors (HBDs).

The vibration levels of the two inactive bearings were at or slightly above the preliminary threshold, indicating that the bearings are healthy or might contain minor defects. Visual inspection revealed a small, repaired spall on the inboard cone of bearing L4, which explains the vibration levels being slightly above the preliminary threshold for that bearing. Overall, the temperature and vibration profiles of the inactive bearings did not exhibit any abnormal behavior throughout the duration of test.

### 4.2 Experiment 283A

After eight days of testing, grease leakage was observed in small quantities from the inboard seal of bearing L2, as shown in Figure 31 and Figure 32. Less than one week later, grease leakage was also observed from the outboard side of bearing R2, as illustrated in Figure 33. The leakage persisted throughout the test and gradually decreased to a few drops near the end of the test, as documented in Figure 34 through Figure 42. Aluminum plates and tarps were installed to collect the leaking grease for analysis.

Post-test inspection revealed that the seal weld was located approximately 140° from the region of the grease leak for the inboard and outboard L2 seals and the inboard R2 seal, as depicted in Figure 98 through Figure 106. This observation suggests that the seals appear to be compromised after extended inactive periods under load, resulting in grease leakage.

Figure 28 and Figure 29 show that bearing R2 consistently operated at higher temperatures than bearing L2 throughout the test. Moreover, both inactive bearings, L2 and R2, operated at higher temperatures than the control bearings on the same axle by an average of 16°C (28.8°F) and 25°C (45°F), respectively. Nonetheless, the operating temperatures of both inactive bearings remained within the typical range for

healthy bearings under the same speed and load conditions and were well below the AAR recommended alarm threshold for HBDs.

The vibration levels of bearing R2 were at or slightly above the preliminary threshold, indicating that the bearing was either healthy or contained only minor surface damage. Visual inspection revealed a small spall measuring 3.87 mm<sup>2</sup> (0.006 in<sup>2</sup>) on the inboard cone of bearing R2, which is consistent with the minor increase in vibration levels around 1300 hours, as shown in Figure 28. Bearing L2 also exhibited vibration levels suggestive of potential spall development. However, subsequent investigation found that the accelerometer calibration was incorrect, resulting in artificially elevated vibration levels. The faulty accelerometer was replaced and the subsequent bearing vibration level measured 2 G<sub>RMS</sub>, indicating that no spall had developed.

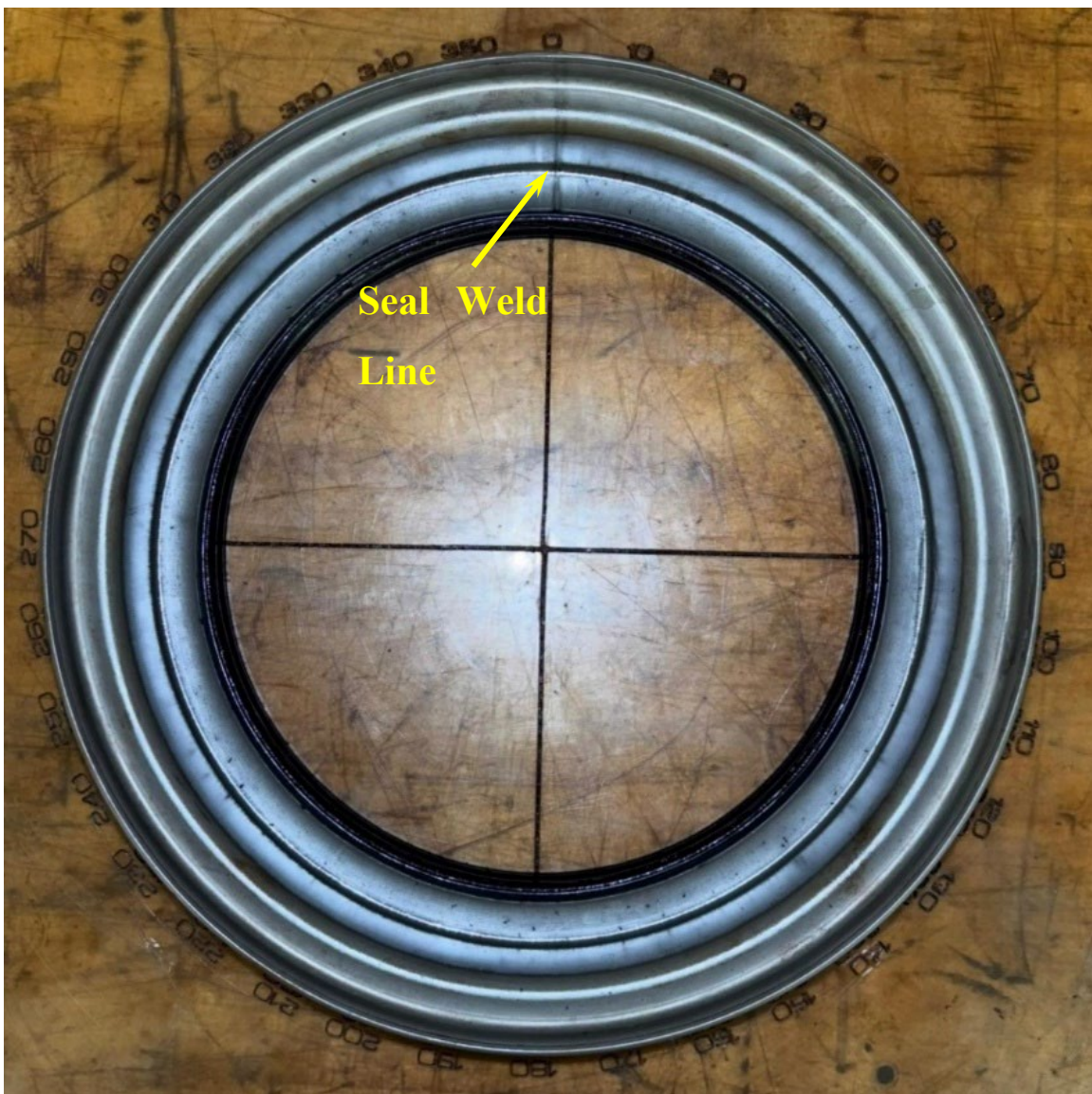


Figure 98: Overview of Bearing L2 OB seal



Figure 99: Seal weld line of Bearing L2 OB seal



Figure 100: Grease leak area of Bearing L2 OB seal



Figure 101: Overview of Bearing R2 IB seal



Figure 102: Seal weld line of Bearing R2 IB seal



Figure 103: Grease leak area of Bearing R2 IB seal



Figure 104: Overview of Bearing R2 OB seal

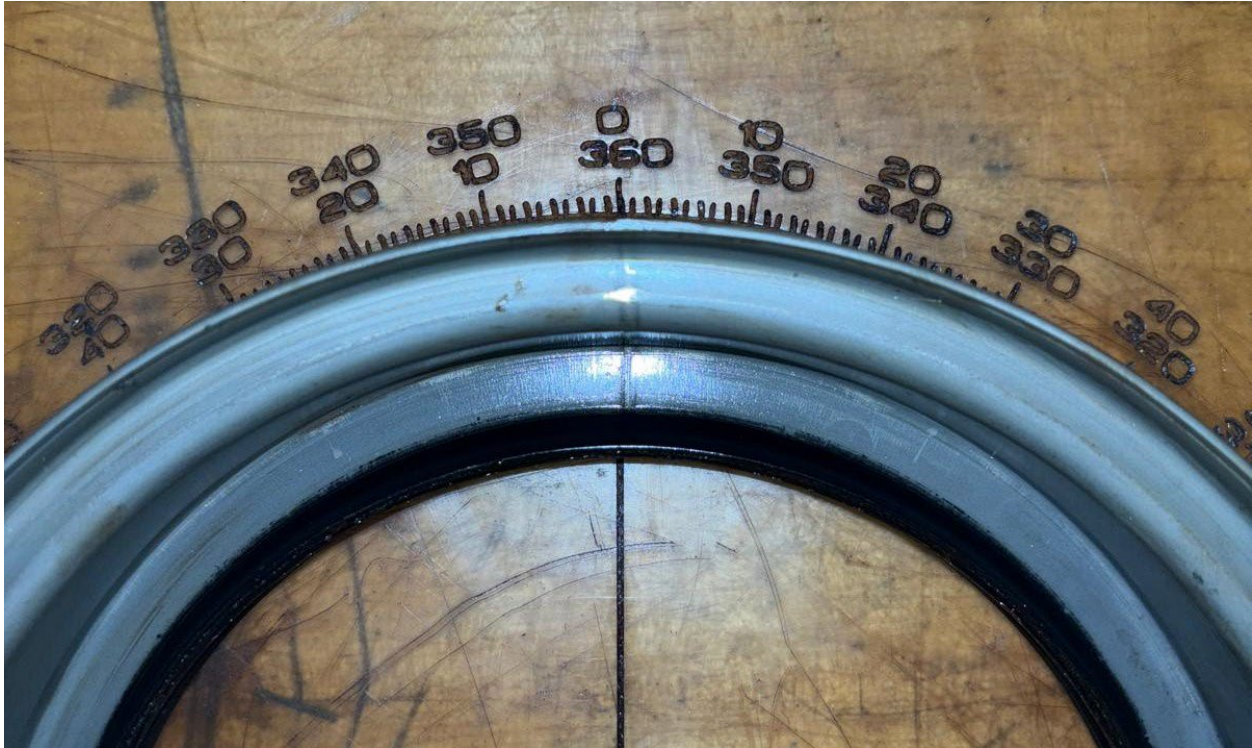


Figure 105: Seal weld line of Bearing R2 OB seal



Figure 106: Grease leak area of Bearing R2 OB seal

#### 4.3 Experiment 304A

The temperature and vibration behavior of the inactive bearings (B2 12-Month and B3 6-Month) exhibited similar patterns early in the test, as shown in Figure 61. Prior to the data-collection interruption, both bearings operated at temperatures comparable to the control-bearing correlation under full-load conditions.

After data collection resumed, the 12-Month bearing operated at noticeably higher temperatures than the 6-Month bearing and the control bearings. It is important to note that the 6-Month bearing also ran slightly warmer than the control bearings but remained within the normal operating range.

The vibration data for the 12-Month bearing showed a gradual trend upwards, with vibration levels increasing from approximately 3  $G_{RMS}$  to 5  $G_{RMS}$  during the mid-portion of the test. Vibration levels continued to rise rapidly toward the end of the test, reaching about 11  $G_{RMS}$  before the test was terminated. These elevated vibration levels exceeded the maximum threshold for healthy bearings and are indicative of defect initiation and subsequent progression.

The temperature profile for the 12-Month bearing showed a corresponding upward trend. During operation at 35 mph (56 km/h) and 17% load, the operating temperature averaged approximately 15°C (27°F) above ambient. Under full-load conditions, temperatures averaged about 50°C (90°F) above ambient until data collection was interrupted by the LabVIEW error described in Note 1. When data collection resumed, the 12-Month bearing exhibited substantially higher temperatures than those observed earlier in the test. Temperatures remained near 70°C (126°F) above ambient for several hours before rapidly increasing to a maximum of 98.6°C (178°F) above ambient prior to shutdown. Cup indexing (i.e., the bearing outer ring or cup, which is supposed to remain stationary, was rotating under full applied load) was observed shortly before the test was terminated, further confirming abnormal operation. This maximum temperature exceeded the AAR recommended hot-bearing detector alarm threshold.

In contrast, the 6-Month bearing exhibited stable vibration and temperature behavior throughout the test. Vibration levels increased gradually from approximately 1.8  $G_{RMS}$  to 2.8  $G_{RMS}$  and remained near this range for most of the test, with a minor increase to approximately 3.6  $G_{RMS}$  near the end. This increase is attributed primarily to crosstalk from the adjacent 12-Month bearing, which was noticeably loud at that stage of the test. These vibration levels were slightly above the preliminary threshold (~2.9  $G_{RMS}$ ) but remained well below the maximum vibration level limit for healthy bearings. The temperature profile of the 6-Month bearing remained stable before the data-collection interruption and averaged approximately 51°C (92°F) above ambient after data collection resumed.

In summary, the 12-Month bearing experienced a progressive increase in both vibration and temperature, followed by an abrupt rise near the end of the test, consistent with spall initiation and subsequent growth. Conversely, the 6-Month bearing exhibited normal operating behavior, with only minor increases in vibration and temperature remaining within acceptable healthy limits.



Figure 107: Comparison of the IB cone assembly (left) and OB cone assembly (right) for the B2 (12-Month) bearing

Figure 107 contrasts between the state of the grease on the inboard (IB) cone assembly, which had no discernable raceway damage, and that of the outboard (OB) cone assembly, which exhibited significant damage that spanned 58% of its total raceway surface area.

#### 4.4 Experiment 304B

The bearing exposed to approximately six months of outdoor environmental conditions (B3) completed the target mileage without any abnormal behavior.

As shown in Figure 87, the vibration levels for the 6-Month bearing remained near or below the preliminary threshold for the majority of the test duration. During approximately the final 50 hours of operation, the vibration levels increased slightly and intermittently exceeded the preliminary threshold. However, the increase was minor, did not exhibit a sustained upward trend, and remained well below the maximum threshold for defective bearings.

The temperature profile of Figure 87 indicates that the bearing operated within the typical temperature range for healthy bearings under the same speed and load conditions throughout the test. No abnormal temperature rise was observed, and the operating temperature remained well below the AAR recommended Hot Bearing Detector (HBD) alarm threshold of 94.4°C (170°F) above ambient.

Following completion of the target mileage, a full teardown and visual inspection of all four bearings was performed. Inspection of the 6-Month bearing revealed a shallow superficial scratch on the outboard cup raceway. Slight roller-width discoloration was observed on the inboard cone raceway. No evidence of spall formation or progressive raceway damage was observed.

Overall, the vibration and temperature behavior of the 6-Month bearing remained stable throughout the test, and the bearing successfully reached the target mileage under sustained full-load conditions and 66 mph (106 km/h).

## 5 Grease Analysis Methods

Grease analysis was conducted as part of the broader inactivity study to evaluate changes in lubricant condition associated with extended idle storage. Grease samples were collected from inactive bearings and analyzed using thermal, tribological, and statistical methods. The results presented in this section complement the mechanical performance testing and post-test inspections previously discussed in this report.

### 5.1 Grease Sampling

Grease samples analyzed in this study were obtained from inactive bearings that were either opened upon receipt at UTRGV or disassembled following performance testing on the UTCRS four-bearing test rig. Bearings were labeled according to their original railcar location and axle orientation.

Grease sampling of the bearing components was conducted to identify any localized degradation or uneven protection that might contribute to early failure due to prolonged inactivity. The grease samples were taken from eight different sections of the bearings. A representative depiction of these sections can be found in Figure 108, where the labels correspond to that of the left bearing on axle 4. Grease was collected from both the loaded ( $90^\circ$ ) and unloaded ( $270^\circ$ ) sides of: the seals and spacer ring (loading orientation depicted in Figure 108), and from the cones. These locations were selected to gauge differences in thermal and tribomechanical history that occurred during operation as well as to ascertain the effects of inactivity. Grease samples were collected in resealable glass vials to minimize oxygen exposure after collection.

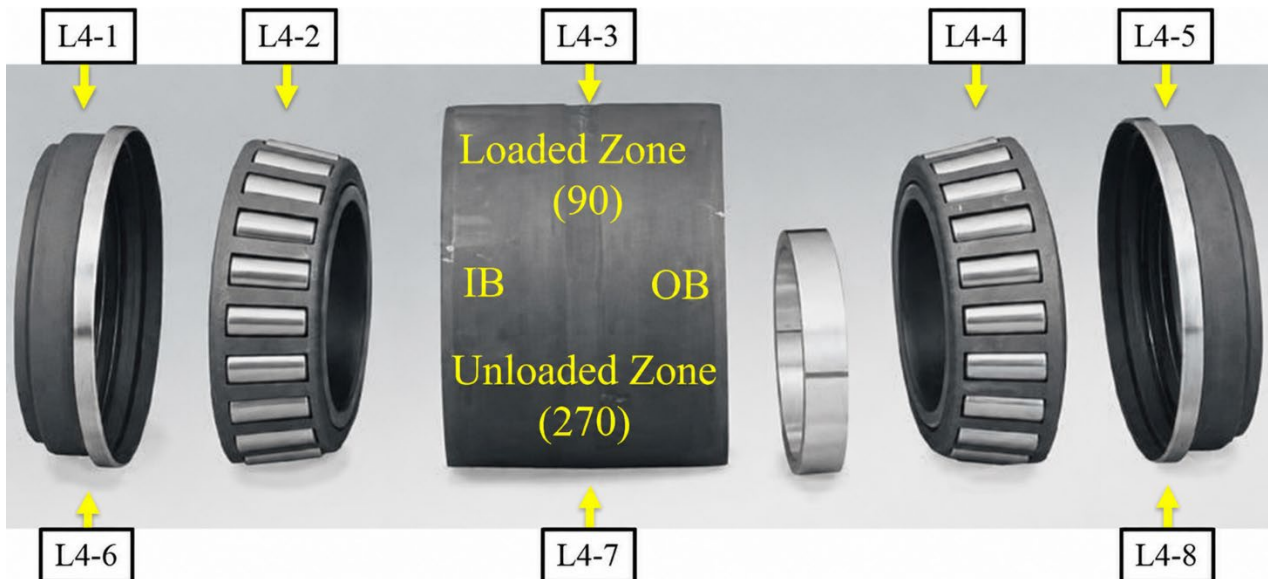


Figure 108: Exploded view of tapered roller bearing with grease sampling labels (Left Bearing on Axle 4)

## 5.2 Thermal Analysis (DSC and TGA)

Thermal characterization of the grease samples was performed using a Differential Scanning Calorimeter (DSC) and a Thermogravimetric Analyzer (TGA). The DSC is an analytical instrument which measures the difference between the heat flow into a sample pan and an empty reference pan as the chamber is exposed to some heating profile. An oxidation induction time (OIT) test was performed in the DSC, where the sample was rapidly heated to and held at 210°C (410°F) in a nitrogen-filled environment before the purge gas was switched to air. At this point, the oxygen in the purge air will react with antioxidants in the grease. While antioxidant additives are active, the underlying hydrocarbons will not oxidize. Once the protective additives are consumed, decomposition of the oil component of the grease begins, resulting in an exotherm (upward shift) in the heat flow. The time for decomposition to begin is called the oxidation induction time (OIT), hence the OIT test. For comparison, one of the commonly approved greases for rail service has an OIT when new of at least 40 minutes.

Analysis of the DSC trace also allows for the determination of the thermal decomposition energy (TD) of the lubricating oil component of the grease by integration of the exotherm peak. The TD is a measure of the remaining lubricant in the sample. Representative example plots of these analyses are shown in Figure 109.

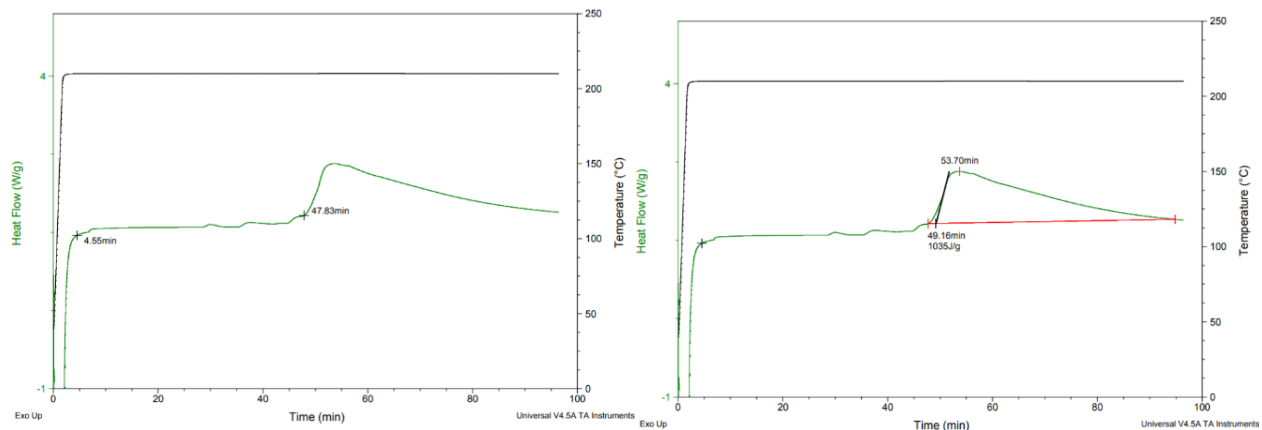


Figure 109: DSC Graphs demonstrate the OIT (left) and the TD (right) of new grease

Thermogravimetric Analysis (TGA) is a technique which measures change in mass of a material as it is subjected to a controlled temperature program that typically involves heating, cooling, or isothermal holds. A series of drops in weight and varying temperatures can be observed when analyzing lubricating grease. The first observed drop in weight is associated with the decomposition of lighter lubricating molecules. Later drops are associated with thickeners and other components of the grease. The TGA is able to detect and quantify entrained moisture as that will vaporize well below the oil decomposition temperature.

Sample masses of 7 mg per specimen were tested using ceramic pans that permitted heating rates of 10°C per minute until a final temperature of 800°C (1472°F) was reached. An example TGA scan is presented in Figure 110.

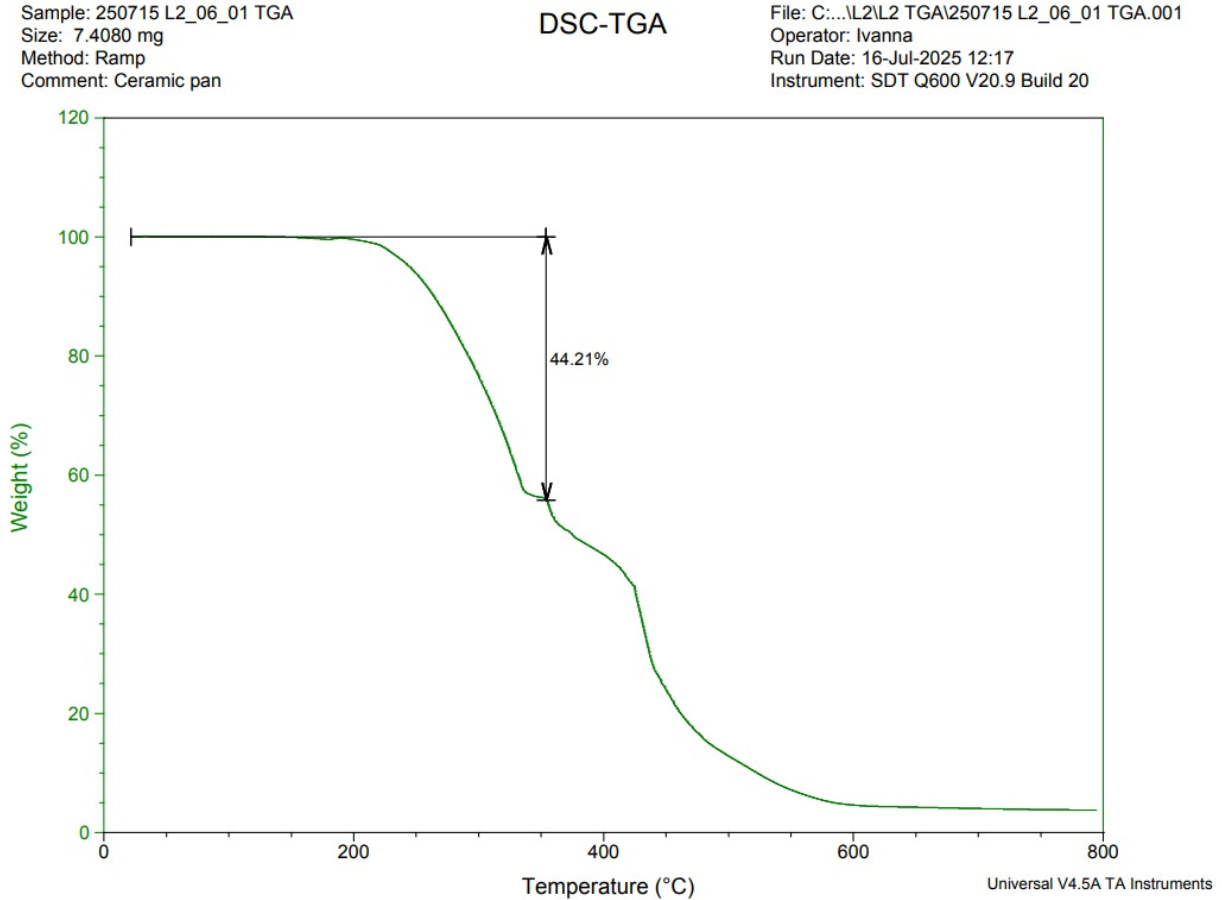


Figure 110: Sample TGA output depicting first decomposition step

### 5.3 Tribology Testing

The tribological evaluations were conducted using a DUCOM Four Ball Tester (FBT-3) following a modified version of the ASTM D-2266 standard. The test utilized chrome steel balls (AISI 52100 steel, 60 HRC hardness, 0.5-inch diameter) at a speed of 1450 rpm and a load of 1200 N. Tests were run for 5 minutes at 24°C. This testing system operated with three stationary steel spheres positioned at the bottom and a single rotating sphere on top that spun at a specified speed while all are immersed in the lubricant. Each test required approximately 15 grams of the grease sample. During the test, the frictional torque required to rotate the system was recorded, and after testing, the diameter of the resulting wear scar (WSD) was measured on each of the steel spheres.

## 5.4 Statistical Analysis

Analysis of the effects of inactivity is somewhat constrained as the operational histories prior to the extended period of inactivity of the bearings were unknown. One possible comparison that can be made involves bearings on the same axle. These pairs are likely to have had similar operational histories; however, differences in lubricant condition are possible due to the following factors: differences in micro-climate on opposite sides of the car, such as different exposure to sunlight, longer dew residence times, severe freeze-thaw cycling, and/or higher humidity due to proximity to a body of water. Independent analysis of different regions of a bearing may also be used to identify the effects of prolonged inactivity, as the various locations potentially experience differing thermal, tribomechanical, and oxygen exposure histories.

Due to the complexity of the available data, R software, a statistical computing software, was used to develop a regression model for each of the three response variables: OIT, decomposition energy (TD), and weight loss. There are four variables that capture the environment of the stored railway bearings: Axle, Side, Maj Loc, and Angle. These four variables will serve as the regressors or factors for the regression model and all four regressor variables are categorical. Categorical data consists of names or labels and involves the use of data tables and is always discrete. On each axle, there were two bearings, labeled as Side, with the name varying per location on the axle. In the model, they are nested within the axle and, as such, must be properly embedded in the model formulation. Within each bearing, there are two factors: location (Maj Loc), which is the variable representing the subcomponents, and angle, which refers to the loading position. Both factors are nested within the bearing. The model is formulated in such a way that it is a three-stage nested hierarchy with crossed fixed effects to filter out the non-hierarchical data [4]. A linear mixed-effects model was selected as it is commonly associated with three-stage nested designs that include crossed effects [5]. For this study, the variables Axle and Side were random effects that account for variability. The variables Maj Loc and Angle were fixed effects terms.

Additionally, this data can be described as “messy.” There are missing values for Wt\_Loss, the variable assigned for the weight loss. When examining the variable Maj Loc, there are 20 observations for raceway, 24 observations for spacer, and 40 observations for seal. A similar situation applies to variables Axle and Angle. This data set is said to be unbalanced because the number of occurrences of combinations of variables is not the same for all combinations. Traditional factorial designs are balanced so traditional analysis is not possible and the presence of missing and unbalanced data had to be considered when fitting the model. The regression model that contains missing and unbalanced data uses a restricted maximum likelihood method, a statistical method that provides less biased estimates of variance components, to fit the linear mixed-effects (regression) model. The relevant code for this analysis in R is shown in Figure 111 for the OIT data.

```
model12 <- lmer(OIT ~ `Maj Loc` * Angle + (1 | Axle / Side),
  data = InactiveBearingGrease,
  REML = TRUE)
```

Figure 111: R Code for analysis of OIT

## 5.5 Results and Discussion

### 5.5.1 Grease Analysis

A total of 84 separate samples from ten paired bearings were evaluated for OIT, decomposition energy, and weight loss. The regression model was applied first to the entire dataset, which included both the four as-received bearing samples and the six which were subjected to performance testing. The initial model showed significant differences between OIT values and weight loss between the axles, which is expected since they had differing service histories prior to the inactive period. Also of note is that differences between bearings on the same axle were insignificant, implying uniform prior history for those paired bearings. There was a significant ( $p = 0.045$ ) difference in the OIT between the grease in the raceway or seal areas compared to the spacer region. This is consistent with behavior observed in prior work [6] [7]. The regression model indicates that there is no statistically significant difference in the condition of the samples from the seals and the raceways. Because there was no significant difference between those locations, the values have been averaged in Table 19. It should also be noted that TGA weight loss data showed no evidence of significant water contamination in the tested samples.

Table 19: Average OIT, TD, and Weight Loss Values Using Raceway and Seal Samples

Axle		Left Bearing		Right Bearing	
		Top (90°)	Bottom (270°)	Top (90°)	Bottom (270°)
1	Avg. OIT [min]	10.1	9.3	15.5	15.4
	Avg. TD [J/g]	1596	1309	1288	1637
	Avg Wt. Loss [%]	62.5	61.2	61.4	62.0
7 (run)	Avg. OIT [min]	0.0	0.0	0.0	0.0
	Avg. TD [J/g]	1989	2047	1477	1577
	Avg Wt. Loss [%]	60.7	56.5	49.9	49.4
8	Avg. OIT [min]	0.0	0.0	0.0	0.0
	Avg. TD [J/g]	1020	1320	1195	1435
	Avg Wt. Loss [%]	48.4	49.8	50.7	49.7
4 (run)	Avg. OIT [min]	3.1	2.2	2.3	2.2
	Avg. TD [J/g]	1712	2011	2329	2276
	Avg Wt. Loss [%]	42.9	46.9	43.7	42.9
2 (run)	Avg. OIT [min]	2.4	2.4	2.8	2.5
	Avg. TD [J/g]	1769	1686	1833	1896
	Avg Wt. Loss [%]	42.8	42.8	43.2	43.1

Of particular note are the zero OIT values from axles 7 and 8, as this indicates that the history of those bearings has completely consumed the antioxidant package, so the oil in those bearings will oxidize or has already begun to oxidize as conditions warrant.

The regression analysis was rerun with just the four untested bearing results (i.e., axle 1 and 8 bearings) because of the potential for mixing in the tested bearings (i.e., axle 2, 4, and 7 bearings). The analysis showed no statistically significant differences (Figure 112) for any of the results. These results indicate that significant separation of oil has not occurred during the inactive period. Both the weight loss and the decomposition energy results indicate no consistent change in oil content between the loaded (top portion) and unloaded (bottom) regions of the bearings.

Fixed effects:						
##	Estimate	Std. Error	df	t value	Pr(> t )	
## (Intercept)	5.7125	6.3156	1.0086	0.905	0.531	
## MajLocC	0.6912	0.5469	19.0046	1.264	0.222	
## Angle90	0.4567	0.5795	19.0049	0.788	0.440	
## MajLocC:Angle90	-0.2967	0.7316	19.0048	-0.406	0.690	

Figure 112. Sample Output from Statistical Model for Decomposition Energy

One potential limitation of this analysis is that the quantity of material used in each test is small. Though samples were mixed thoroughly before test specimens were collected, there is the potential for increased variability between specimens due to inhomogeneity in the partially degraded grease. However, the four ball wear test uses a larger specimen size and should thus not suffer from this possible issue.

### 5.5.2 Four Ball Wear Testing

The following table includes wear scar diameter (WSD) data and frictional torque values for each grease sample tested using the DUCOM Four Ball Tester. Due to the greater volume of grease required, not all grease samples could be tested. The reference material (Ref.) was fresh grease of the type most likely to have been used in the bearings received. The tested samples are identified according to the same conventions used in the thermal analysis. Each test run produced wear scars on three balls, so a single test provided three WSD values, which were then averaged. Only one frictional torque was measured per test.

Table 20: Tribological Evaluation Results

Sample	Bearing	WSD [μm]	Avg. WSD [μm]	WSD Std. Dev. (σ) [μm]	Avg. Std. Dev. (σ) WSD [μm]	Frictional Torque [N·m]	Avg. Frictional Torque [N·m]	Std. Dev. (σ) Frictional Torque
Reference	Ref. (1)	1695	1678	15	16	0.347	0.362	0.0139
		1673						
		1666						
	Ref. (2)	1735	1732	10				
		1721						
		1741						
	Ref. (3)	1699	1715	23				
		1705						
		1741						
Top Samples	R8-90	2235	2286	48	44	0.353	0.363	0.0089
		2294						
		2330						
	L1-90	1844	1841	61				
		1847						
		1832						
	L8-90	2278	2347	8				
		2370						
		2394						
Bottom Samples	R8-270	2211	2241	33	22	0.356	0.359	0.0055
		2236						
		2276						
	L1-270	1922	1953	27				
		1971						
		1965						
	R1-270	1801	1794	12				
		1801						
		1780						

All of the inactive bearings show inferior wear protection compared to the new grease, consistent with expectations for grease which has seen significant service. There does not appear to be a statistically significant change in wear scar diameter with respect to sample location (top or bottom) on the bearing. Further, the variation in performance of the prior service greases is greater than the variation in the new grease. Further statistical analysis as well as profilometric characterization of the wear areas are in progress.

## 6 Conclusions and Future Work

This study represents a systematic evaluation of railroad bearing performance following extended periods of inactivity. The study was motivated by research need statements from the railroad industry and the NTSB following the East Palestine, OH, train derailment, in which the culprit bearing had experienced two prolonged idle periods of 565 days and 216 days. The results presented herein include findings from the laboratory testing performed on the second and third sets of inactive bearings received from a Class I railroad, as well as two bearings that underwent a 6-month and a 12-month outdoor exposure study. Moreover, the thermal analysis conducted on the lubricating grease from the long-term inactive bearings is also presented. As this study is still in its early stages and based on a limited sample size, the authors caution against generalizing these results.

The second and third sets of inactive bearings operated without notable incident, aside from losses of initial grease content. Bearings R4 and L4 lost approximately 2.2% of their initial grease quantity, while bearings R2 and L2 lost 14.5% and 10.9%, respectively. A small divot observed on the inboard cone of bearing L4 was attributed to prior reconditioning rather than natural spall formation, while a small spall measuring approximately 0.006 in<sup>2</sup> (0.015 mm<sup>2</sup>) was identified on the inboard cone of bearing R2. For all inactive bearing tests, operating temperatures remained within the range of typical healthy bearings under comparable speed and load conditions and well below the AAR-recommended HBD alarm threshold.

The 12-month exposed bearing (B2) exhibited elevated vibration and temperature behavior, culminating in the formation of multiple spalls on the outboard raceways and the onset of cup indexing under full applied load prior to shutdown. Moreover, the operating temperature for this bearing exceeded the AAR recommended alarm thresholds for HBDS. In contrast, the 6-month exposed bearing (B3) operated within normal limits, with only minor increases in vibration and temperature and concluded the 100,000-mile testing protocol with no incidents. These findings suggest a potential relationship between extended idle periods and the onset of raceway surface degradation once bearings are returned to service.

A high incidence of lubricant leakage was observed in inactive bearings, suggesting a potential degradation of seal integrity. Such leakage has not been previously observed at the UTCRS, even in bearings subjected to extended service experiments. Service life testing of bearings exposed to direct sunlight to simulate thermal cycling further supports this observation.

Thermal analysis of lubricating grease from bearings idled for more than three years revealed a weak significant difference ( $p = 0.045$ ) in OIT between grease sampled from the raceway and seal regions and grease sampled from the spacer region, with shorter OIT values measured in the raceway and seal areas. This behavior is consistent with differences in oxygen availability, thermal exposure, and metal debris generation in these regions and is not necessarily attributable to the bearing inactivity. This result is

consistent with previously published work based on larger populations of laboratory-tested bearings with known operational histories [6] [7].

Grease samples obtained from the upper portion of the bearing (loaded region) were not statistically different in decomposition energy or weight loss from those taken from the lower portion (unloaded region). Because both measures are proxies for oil content, this indicates that separation of grease constituents during extended idle periods either does not occur or cannot be detected by these methods. The consistency of performance of lower and upper samples in the four-ball wear test, which uses more grease for each test, also indicates that there is no significant difference that can be attributed to the separation of the lubrication components. Thus, this study found no clear evidence of significant separation of the grease during extended idle periods. Earlier work, which was based on a preliminary set of tests, showed some difference between specimens from the top and bottom of the bearing, but a complete test array showed that the apparent difference disappeared with a larger test set.

No statistically significant differences were observed between left- and right-side bearings on the same axle, suggesting that micro-climate variations were not significant for these cars and supporting the conclusion that paired bearings shared similar operational histories.

In summary, thermal analysis and four ball testing of grease samples suggest that inactivity does not result in obvious changes to the lubricant. No other observed changes in grease condition could be definitively attributed to inactivity. Reductions in OIT, along with decreases in weight loss and decomposition energy, are reasonably consistent with normal service conditions.

As part of the third-year project, test bearings have been placed in an exposed location on the laboratory roof, and grease samples are periodically taken for thermal and viscosity analysis. This extended study will provide information about lubricant changes where the full history of the bearing and lubricant is known.

## 7 References

- [1] C. Tarawneh, A. Blanton, M. Adame, A. Martinez. Effect of Long-Term Inactivity on Railcar Bearings – Year 1. Report No. UTCRS-UTRGV-M4CY23, September 2024.  
<https://www.utrgv.edu/railwaysafety/research/mechanical/index.htm>
- [2] C. Tarawneh, J. Lima, N. De Los Santos, R. Jones, 2019, “Prognostics models for railroad tapered-roller bearings with spall defects on inner or outer rings,” *Tribology Transactions*, Vol. 62, No. 5, pp. 897-906.
- [3] C. Tarawneh, J. Montalvo, and B. Wilson. Defect detection in freight railcar tapered-roller bearings using vibration techniques. *Railway Engineering Science*, 29(1): 42-58, 2021.  
<https://doi.org/10.1007/s40534-020-00230-x>
- [4] Montgomery, D. C. (2019). *Design and Analysis of Experiments* (10th ed.). Wiley Global Education US. <https://bookshelf.vitalsource.com/books/9781119492443>
- [5] ImerTest-package function - RDocumentation. (2017). Rdocumentation.org.  
<https://www.rdocumentation.org/packages/ImerTest/versions/3.1-3/topics/ImerTest-package>
- [6] Timmer, D., Jones, R., and Tarawneh, C., "Modeling the Useful Life of Railroad Bearing Grease," 2014 Informs Conference, San Francisco, CA, November 9-12, 2014.
- [7] Timmer, D., Martinez, T., Jones, R., and Tarawneh, C. “Models for the Residual Life of Railroad Bearing Grease in Laboratory and Industry Applications,” *Proceedings of 2017 ASME Joint Rail Conference*, Philadelphia, PA, April 4-7, 2017.